PNAS
www.pnas.org

Supplementary Information for

Cultivar diversity buffers winegrowing regions from climate change losses

I. Morales-Castilla, I. García de Cortázar-Atauri, B.I. Cook, T. Lacombe, A. Parker, C. van Leeuwen, K. A. Nicholas, and E.M. Wolkovich

Corresponding Author Ignacio Morales-Castilla.
E-mail: ignacio.moralesc@uah.es

This PDF file includes:

Supporting Information Text

Data

Phenological data for parameterization & validation
We assembled historical data for 50% budbreak, 50% flowering and 50% veraison dates from 62, mostly French, locations between 1956 and 2015 (see list of data sources in Table S1). Most observations are for the 1995-2007 period and secondarily the 1975-1994 period. The dataset includes 517 observations of budbreak, 757 observations of flowering and 688 veraison observations. Requirements for phenological observations were: budbreak was identified as stage 4 on the modified Eichhorn and Lorenz (E-L) scale (1); flowering was identified as the 50% flowering date corresponding to stage 23 on the modified E-L scale; veraison corresponded to stage 35 on the modified E-L scale where 50% of berries softened or changed from green to translucent for white cultivars, or changed color for red cultivars. These data represent a portion of the the original database collected in Parker *et al.* (2), which was subsequently released for use within this project, and include matched local meteorological data.

Our phenology dataset included data for 11 common winegrape cultivars (varieties): Cabernet-Sauvignon, Chardonnay, Chasselas, Grenache, Merlot, Monastrell (syn. Mourvedre), Pinot noir, Riesling, Sauvignon blanc, Syrah and Ugni blanc. These varieties were selected based on their widespread cultivation (all are globally planted and many are considered international varieties, 3, 4), and ensuring that the set of selected varieties encompassed representative phenological diversity (Fig. S4). All are 100% *V. vinifera* subsp. *vinifera* varieties.

The above-described phenology dataset was utilized to parameterize models designed to forecast phenology across space and time, and then validate them via cross-validation methods (see *Methods* below). To further validate phenological models we used data independent from the data used to parameterize the models. We assembled a validation dataset of phenological observations from the following sources: (a) published articles on winegrape phenology containing observations for budbreak, flowering and veraison (i.e., 5–7); (b) phenological observations extracted from a report sponsored by the Napa Valley Vintners (8) (see https://napavintners.com/about/docs/nvv_climate_exec_summary.pdf; data not publicly available); and (c) our own phenological data collected at the University of California, Davis (9). These data sources comprise a dataset for five sites (which we refer to as the 'independent validation dataset'), containing all analyzed varieties except for Grenache, and included observations from 1949 to 2016. Note that the dataset does not contain observations for all varieties and all years in each site (see Table S2).

Finally, we also used phenological data from INRA Domaine de Vassal Grape Collection to put the phenology of our selected cultivars into context by comparing them with a wider diversity of cultivars (130 others, selected to capture major varieties and the phenological diversity of winegrapes). The Domaine de Vassal Grape Collection, currently located in Marseillan-plage (France), is dedicated to the conservation, characterization and valorization of grapevine genetic resources. As such it grows many varieties of *Vitis vinifera* subsp. *vinifera* and records phenology relative to a standard variety (Chasselas, 10). For more information visit: INRA Vassal-Montpellier Grapevine Biological Resources Center at www6.montpellier.inra.fr/vassal and French Network of Grapevine Repositories https://bioweb.supagro.inra.fr/collections_vigne/Home.php?l=EN.

Viticulture data—The geography of winegrowing
To analyze climatic suitability in current winegrowing regions we digitized the global distribution of the major winegrowing regions of the world according to a published atlas of winegrowing (11). We considered our results within this limited region (Fig. S1) and, also, all areas our models found were climatically suitable (see below). The dataset on major winegrowing regions is available at https://knb.ecoinformatics.org/view/doi:10.5063/F1SX6BH1 (12).

Climate data
See the main text *Materials & Methods*.

Data availability
Most data used in the paper are already published and publicly-available, including: climate projections (13), historical climate data from BEST http://berkeleyearth.org/data/, winegrowing regions distributions (3, 12), phenological data (2, 5–9); these data can be made available upon request of the authors of each publication. Derived data supporting the findings of this study are available from the corresponding author upon request.

Methods

General workflow & rationale
To forecast winegrape phenology we followed a multi-step procedure. In our first step, using our phenological dataset (Table S1) and BEST climate data, we parameterized phenological models for 11 winegrape varieties. (Note that we did not find major differences between models based on BEST data compared to the meteorological observations, see Table S6.) We chose BEST to parameterize the phenological models for several reasons. First, BEST is one of the few datasets that provide global, gridded, and quality-controlled estimates of daily maximum and minimum temperatures—i.e. using daily temporal resolution is a requirement for our phenological models. Second, the BEST data are gridded at a similar resolution to the LENS, facilitating

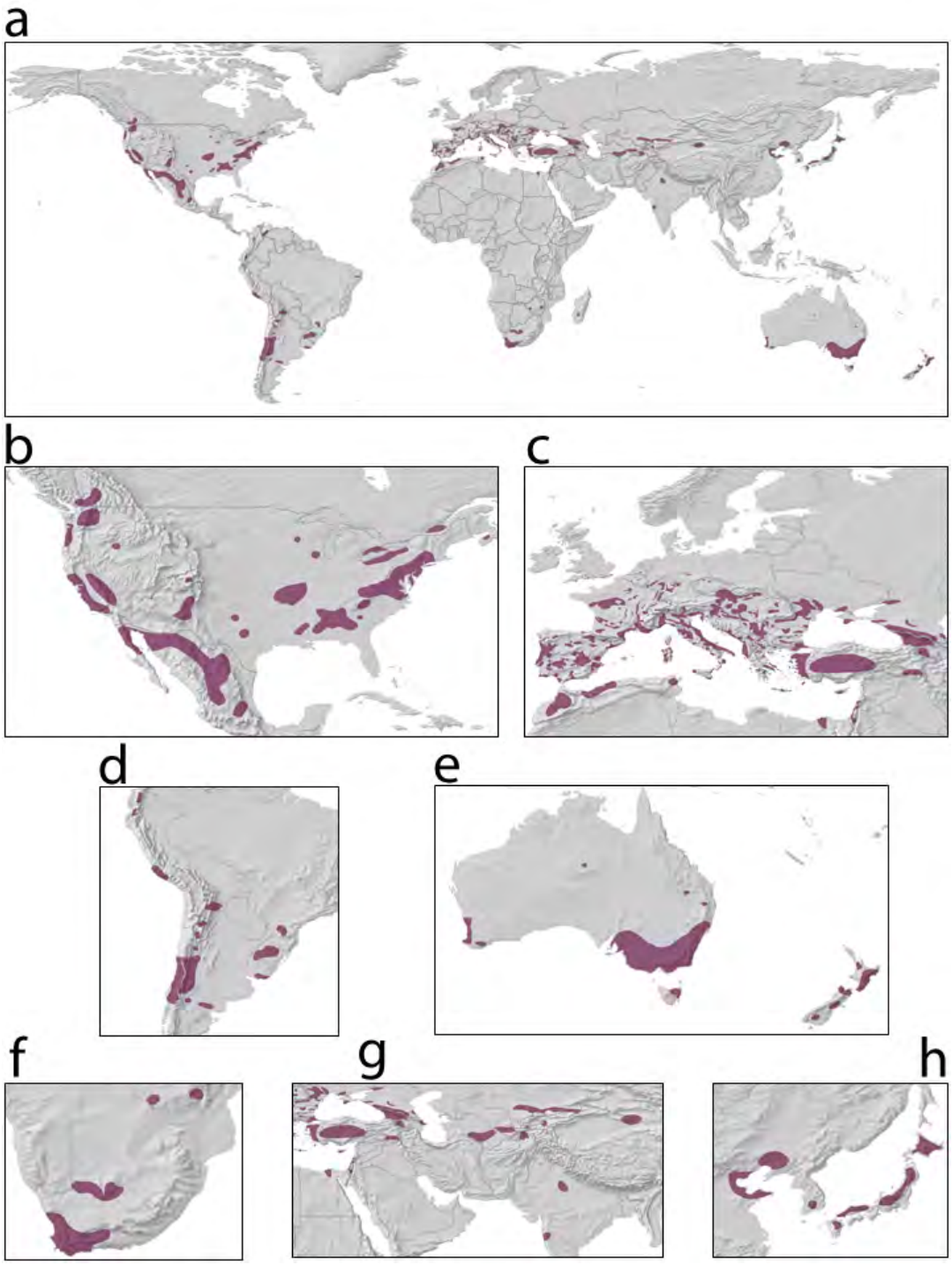

Fig. S1. Maps of current major winegrowing regions of the world (digitized from (11)). The panels show the distribution of winegrowing regions globally (a), in North America (b), Europe and Northern Africa (c), South America (d), Australia and New Zealand (e), Southern Africa (f), Southeast Europe, Middle East and South Asia (g), and Eastern Asia (h). Winegrowing regions are shaded in purple. Note that the map is not comprehensive, it lacks regions developed after 2007 and that some regions depicted only have marginal winegrape production (e.g., southeastern US, central Mexico, areas of Mongolia, north island of Japan).

1) straightforward bias correction of the model climate information and 2) re-gridding of the BEST datasets to the same spatial resolution as the LENS climate projections. We fitted phenological models to estimate the dates at which budbreak, flowering and veraison occur, sequentially—i.e. each phenological stage starts on the predicted date for the preceding stage. In our second step, we validated the models by comparing results of observed vs. modeled winegrape phenology for each stage, variety and region (using the independent validation dataset described above). In our third step, using the validated models, we projected phenology through to veraison for all 11 varieties during our reference scenario (0°C), and the two warming levels of 2°C and

4°C (see *Climate data*; Fig. S5). Finally, we used bioclimatic niche models to predict the climatic suitability to reach maturity of each variety in each region and during the 45 days following veraison (more details given below in *Modeling maturity*). Given these results we could then compare predictions for the climatic suitability of each variety across sites and warming scenarios.

Modeling multiple varieties' specific responses to future climate has two major advantages for growers. First, beyond forecasting geographic shifts in climatic suitability for viticulture, which has already been done (e.g., 14, 15), it allows establishing which particular regions will become most suitable to grow which variety. This information could guide a grower's decisions by, for example, focusing on a popular variety such as Pinot noir, and forecasting whether the grower's land will present suitable conditions to grow it under different warming scenarios (Figs. 1 and S13). While this approach has been done previously for a single variety (e.g., 16), it is rarely done for more than one at a time (but see 17, for an example using growing season mean temperatures). Second, having multiple variety-specific results allows us to build variety diversity maps (Figs. 1b and S13b). These maps yield more explicit information of the potential of winegrape diversity with climate change: the more varieties forecasted to reach maturity in a given region, the more resilient that region will be to losing climatic suitability for viticulture. Finally, modeling multi-variety responses to climate change is required to quantify the adaptive potential of within-crop agrobiodiversity.

Phenological modeling

We modeled winegrape phenology for each of the 11 varieties according to a phenological process-based model (which treated each stage sequentially), considering only pixels where each 10-year scenario had no more than two days below -20°C or one day below -30°C (18, 19). Freezing temperatures below -20°C have been shown to generate tissue damage in grapevine (18), and thus, these thresholds are necessary because as climate warms high latitude locations are predicted to start providing the necessary heat during the growing season for winegrowing, but winters may still be too cold.

Our approach combined model estimates of three key stages of grapevine development: budbreak, flowering and veraison. The budbreak stage was simulated using a process-based sequential model combining the Smooth-Utah model (20, 21), which simulates dormancy break (accumulating chilling units) and the Wang and Engel model (22), which simulates the post-dormancy phase until budbreak. Then, the Wang and Engel model was used to simulate the accumulation of forcing units until flowering, and after flowering, it was used to simulate accumulation of forcing units until veraison. The curvilinear structure of both the Smoothed-Utah and Wang and Engel models reproduce the known effect of a developmental slowdown at high temperatures (23).

The Smoothed-Utah model (20, 21) assumes that chilling can only occur within a given range of temperatures, and allows for negative chilling in warm days:

$$F_{SmoothedUtah} = \begin{cases} \dfrac{1}{1+e^{-4\frac{T_d-T_{m1}}{T_{opt}-T_{m1}}}} & \text{if } T_d < Tm1 \\ 1+\dfrac{-0.5(T_d-T_{opt})^2}{(T_{m1}-T_{opt})^2} & \text{if } T_{m1} \le T_d < T_{opt} \\ 1-\left((1-min)\dfrac{(T_d-T_{opt})^2}{2(T_{n2}-T_{opt})^2}\right) & \text{if } T_{opt} \le T_d < T_{n2} \\ min+\left(\dfrac{1-min}{1+e^{-4\frac{T_{n2}-T_d}{T_{n2}-T_{opt}}}}\right) & \text{if } T_d \ge T_{n2} \end{cases} \quad [1]$$

Where *Tm1* is decrease in cold efficiency for bud endodormancy, *Topt* is the optimal mean daily temperature, *Tn2* is the temperature with half the efficiency of *Topt* to induce endodormancy, and *min* is the negative impact of high temperatures. This model yields the amount of chill units based on daily temperatures (T_d), which are accumulated until a threshold of accumulated chilling action (C*) is reached defining the end of endodormancy.

The Wang and Engel model (22) belongs to the family of beta functions, is asymmetric and has four parameters:

$$f_{\text{Wang \& Engel}} = \begin{cases} \dfrac{2(T_d-T_{min})^{\alpha}(T_{opt}-T_{min})^{\alpha}-(T_d-T_{min})^{2\alpha}}{(T_{opt}-T_{min})^{2\alpha}} & \text{if } T_{min} < T_d < T_{max} \\ 0 & \text{if } T_d \le T_{min} \text{ or } T_d \ge T_{max} \end{cases} \quad [2]$$

$$\alpha = \frac{ln(2)}{ln(\frac{(T_{max}-T_{min})}{(T_{opt}-T_{min})})} \quad [3]$$

Where $T_{min}, T_{opt}, T_{max}$ represent the minimum, optimum and maximum temperature values, respectively, that are included to calculate the amount of forcing needed until a threshold of accumulated forcing units (F*), is reached for a given phenological event—i.e., budbreak, flowering or veraison—to occur. Following many other crops and approaches in winegrapes (2, 24), we consider $T_{min}, T_{opt}, T_{max}$ to be species-level characteristics and thus define one value for each parameter that is repeated across varieties. This approach is consistent with the observation that the precocity hierarchy across varieties is generally constant

within a site across years (as opposed to shifting as expected if $T_{min}, T_{opt}, T_{max}$ vary strongly across varieties), allows us to compare varieties directly, and prioritizes robustness over precision given our data limitations (i.e., at high temperatures we have very few observations for any one variety). Our estimated parameters (see Tables S4-S6) were in line with values estimated by previous research (25). In our modeling approach here, the thresholds for minimum and maximum temperatures (T_{min} at 0°C and T_{max} at 40°C for the Wang & Engel model) were fixed according to physiological thresholds well-established in the literature of winegrapes (26, 27) and other species (24, 28). We set T_{max} at 40°C after comparison of model fit against models using alternative T_{max} values of 36, 37, 38, and 39°C. Values of T_{max} comprised between 35 and 40°C are common in the literature (26, 27, 29, 30), which often shows a drastic reduction in photosynthetic activity above 40 °C (31–33), and thus in phenological development. We acknowledge that phenological models relying upon threshold parameters such as T_{min} and T_{max} may predict different responses above and below the thresholds—e.g. in our example, forcing units are accumulated at T_{max} of 39.9 but not at 40.1°C. However, research on winegrape physiology seems to support the existence of temperature thresholds above which damage may be too high for further plant development (31–33). As new data becomes available it will be interesting to see how phenological models accommodate uncertainty around their threshold parameters. While T_{min}, T_{opt} and T_{max} were fitted or set at the species level, the accumulated thresholds for chilling (C*) and forcing (F*) corresponding to each phenological stage were parameterized at the variety-level (see Tables S5-S7), thus allowing for phenological variation across varieties.

To evaluate model accuracy and performance we calculated: 1) the root mean square error (RMSE, providing a classical evaluation between observed and simulated values) as described by (34), 2) model efficiency and, 3) we performed a leave-out-one cross-validation calculating RMSEP (root mean square error of prediction) as described by (35, 36):

$$N_{PS}(i) = f(X(i), \theta(i)) \quad [4]$$

RMSE in our approach yields the number of days our predictions deviate from the average observed (thus RMSE = 0 would correspond to a perfect fit).

$$RMSEP = \sqrt{\frac{1}{N}\sum_{i=1}^{N}(N_{PS}(i) - N_{PO}(i))^2} \quad [5]$$

RMSEP represents the quadratic distance between the observed (N_{PO}) and the simulated (N_{PS}) phenological stages (here, budbreak, flowering and veraison). RMSEP and RMSE are calculated the same but the result of the former specifically informs of the error of prediction in the cross-validation and the latter computes the calibration error; f represents the model (Smoothed Utah or Wang and Engel) and $X(i)$ and $\theta(i)$ are the vectors of the input data and parameters for the observation i. As with RMSE, the lowest RMSEP are indicative of higher accuracy.

The model efficiency (37) can be defined as:

$$EF = 1 - \frac{\sum_{i=1}^{N}(N_{PO}(i) - N_{PS}(i))^2}{\sum_{i=1}^{N}(N_{PO}(i) - \overline{N_{PO}})^2} \quad [6]$$

Where $\overline{N_{PO}}$ is the mean value of the observed phenological stages.

Additional accuracy metrics have been proposed to standardize RMSE with respect to the standard deviation of observed values. Here we calculated the Residual Prediction Deviation (RPD), defined as:

$$RPD = \frac{\sqrt{\frac{1}{N}\sum_{i=1}^{N}(N_{PS}(i) - N_{PO}(i))^2}}{RMSE} \quad [7]$$

RPD is applicable to observed and predicted values that are normally distributed, and can increase comparability of metrics such as RMSE. It is also fairly easy to interpret as prediction accuracy increases with increasing RPD (38).

The combination of the above models was selected after rigorous tests of alternative modelling approaches. The alternative models tested for the dormancy phase were the BRIN model (39) and the Chuine model (40); alternative models for post-dormancy included the Richardson model (20) both in its constrained and unconstrained version and the sigmoid model (41). Our choice of the Smoothed Utah and Wang & Engel models for budbreak was made according to accuracy metrics (e.g. RMSE, EF and AIC) showing that their combination outperformed alternative options in terms of fit and parsimony (see Table S3). Although the Smoothed-Utah + Sigmoid combination performed similarly well, we favored the Wang & Engel model as it is more realistic biologically—e.g. it does not accumulate forcing units at temperatures below 0°C. The Wang & Engel model has the additional benefits of reducing uncertainty (42), and being more realistic biologically for budbreak, flowering and veraison by replicating the common plant biology of slowed development at higher temperatures (24, 42). We note that while

this approach may not be perfectly accurate it provides a reasonable trade-off between prediction accuracy, strong physiological foundations and simplicity to upscale computationally.

Following the above described validation metrics, we additionally validated our phenological models against independent observations of winegrape phenology recorded at other geographical locations (e.g. California in the USA, Germany, Portugal, Serbia, see Table S2 for data sources) from the locations where calibration data were extracted (e.g. predominantly France in Table S1; see Tables S8-S9 for validation results). For locations in California, where we had raw data on phenological observations—i.e. yearly values of any phenophase for a given variety—independent validation was straightforward—we calculated the RPD and RMSE based on observed vs. the simulated values by our phenological models. For European locations where we had only the mean ± standard deviation values of observed phenology, validation was restricted to comparing these means and errors to those resulting from our predictions for each given period and dataset (see Table S8).

Our cross-validation and independent validation datasets provide estimates of model uncertainty for our global projections, which encompass many regions for which we did not have phenological data. Our core validation method—cross validation of our main dataset (Table S1)—show RMSE of 5.54 ± 1.64 days and RPD of 2.43 ± 0.84 for BEST climate data (all estimates are mean ± SE unless otherwise noted). These values are well within margins generally considered a good fit (2, 39, 43–45). While we note that growers would benefit from an even lower RMSE, these values are limited by how accurately phenology can be observed, especially when integrating across diverse datasets, as we do here. Moreover, our additional validation with independent observations from North American sites with high resolution data—i.e. yearly observations of each phenophase—showed equal or reduced uncertainty (average RMSE of only 2.55 ± 1.04 days in Napa Valley, see Table S8, and RMSE of 2.50 ± 0.71 days in Davis). Correlations between the phenology simulated by our models and independently observed winegrape phenology were high for both the North American and European locations ($R^2 > 0.98$; see Figs. S6-S8). Even for European locations with low temporal resolution data—i.e. we had only mean and SD of phenology across a set of years—but measuring the same phenophase (i.e., 5, 6), we found that our averaged predictions overlap with average observed values (see Fig. S8). Our independent validation results are, however, inherently limited in their scope—i.e. they are generated for 5 locations where not all modelled cultivars are planted—given the current availability of phenological data across winegrowing regions. Yet we argue that our validation analyses show that our fitted phenological models can predict phenology in other regions accurately enough (Figs. S7-S6) to meet our research goals: compare phenological forecasts across cultivars, regions and warming scenarios.

Modeling maturity

Phenological modeling of winegrape maturity is particularly challenging for several major reasons. First, date of harvest responds to a mix of decisions related to the chemical composition of the berries—e.g. sugars, acids, phenolic content, aroma precursors and aromas—that mainly develop during the veraison to harvest period. Thus, while measures of budbreak, flowering and veraison are strongly related to physiological processes, harvest timing is often closely linked to growers and winemakers' preferences in winestyle, or even historical and cultural determinants. Models of maturity are thus often based on sugar measurements (e.g., 46), but data for such models are extremely limited, and recent studies suggest sugar may change separately from acids and other juice compounds with warming (47, 48). Further, while temperature alone can suffice to model the preceding phenological stages (49), more complex interactions among climatic variables, including those related to vine water status (39, 50), are often needed to correctly characterize winegrape maturation.

Thus, we modeled the veraison to harvest phenophase using bioclimatic envelope models (51, 52) based on 8 bioclimatic variables we expected were relevant globally to grape ripening (see also *Diurnal Temperature Range* below) and the recorded climatic conditions experienced by each variety under pre-climate change conditions. Such models are often used to characterize the climatic niche or climatic conditions under which a studied species can survive.

We used the following set of bioclimatic variables (indicators) known to be relevant for winegrowing:

1. Growing Degree Days (GDD) – defines the accumulation of temperatures during which active grapevine growth is expected. Here we consider only temperatures above 10°C, which is the classical threshold to define GDD in grapevines (53, 54), and calculate it starting from the estimated veraison date.

2. Number of days on which maximum temperatures exceed 40°C (temperature above 40°C) – are generally assumed to severely retard or stop photosynthesis, growth and developmental activity (26, 27, 29, 30).

3. Number of days on which minimum temperatures are below 10°C (number of days below 10°C) – as for the previous indicators we consider there is less photosynthetic activity below 10°C (29, 30).

4. Minimum daily temperatures – minimum temperatures during maturation period are used to describe night temperatures, which are well related to good development of secondary compounds (e.g. aromas and color, 55). For each variety, we recorded the distribution of minimum temperatures corresponding to each day within the 45-day period following veraison, and across the 30-year normal period (1950-1980).

5. Maximum daily temperatures – these values are related to sugar content, acidity degradation, physiological problems and *cooked fruit* aromas (if temperatures are too high, 56, 57). For each variety, we recorded the distribution of maximum temperatures corresponding to each day within the 45-day period following veraison, and across the 30-year normal period (1950-1980).

6. Growing Degree Days above the optimal developmental temperatures. Here we consider 25°C as the base temperature, which is coherent with the optimal value of the phenological models (see *Phenological modeling* above; and (58)).

7. Total summed precipitation (mm) – this value has been often linked to impacts on the final yield, and is associated with pests and diseases (59) but also with overall wine quality (50).

8. Maximum daily precipitation: similar information to total summed precipitation, but also helps differentiate between high precipitation due to many smaller events versus one large precipitation event (calculated as the maximum daily precipitation registered within the 45-day period for each year of the 30-year normal period we considered).

Some of these indicators are known to be collinear—i.e. to varying degrees across the different regions where cultivars are planted—and yet we chose them because they can be linked to particular physiological and developmental processes which are relevant for ripening (see above). We found collinearity to be higher for precipitation indicators (see Table S10) but even so, their relative importance to determine loss of climatic suitability differed significantly for most cultivars (see Fig. S17). We present results for all the variables (and an additional analysis where we include diurnal temperature range, see below) as they are relevant to different aspects of the ripening process (e.g., GDD represents accumulated temperatures over the ripening window while maximum and minimum temperature represent extremes). We note, however, that analyses using only a subset of these variables may find different drivers of climatic suitability (e.g., an analysis with few temperature-related metrics outside of GDD would likely find a greater importance of GDD to climatic suitability). The choice of threshold-based indicators was robust to the specific thresholds used—e.g. the effects of the number of days above 40°C on climatic suitability loss were strongly correlated with the effects yielded by the number of days above 39°C ($R^2 = 0.93$).

The existing winegrowing regions for each of the 11 modeled varieties were extracted from (3) according to the following criteria: 1) a minimum of planted 100 *ha*, thus guaranteeing the ability of those regions to adequately support a given cultivar, 2) the target variety represented at least 2.5% of the total area planted globally for that variety, and 3) to minimize prevalence effects derived from certain varieties being distributed in more locations than others (60), we ensure that each variety was modeled based on a minimum of 20 locations (except for Monastrell, for which n=10) and to avoid over-representation of most common varieties—e.g. Cabernet-Sauvignon—we trimmed down the number of locations to a maximum of 120 (Fig. S10). Finally, we cross-validated the models by re-running the models based on randomized subsampled training (70%) and testing (30%) datasets, and comparing results against observations for the 30-year normal period (1950-1980). Selection of the geographical distribution for each variety could, potentially, improve if quality criteria was utilized (i.e. considering only regions where a given variety is known to produce high quality wines). Such data, however, are not available across all areas where each variety is planted. Our approach is thus conservative in focusing on climatic criteria exclusively: it identifies where a given variety would reach maturity regardless of production or quality criteria.

Our bioclimatic envelope approach characterized the distribution of each of the above climatic variables for each winegrape variety over the 45 days following veraison, given estimates over our 30-year normal period. Certain varieties may show shorter or longer ripening periods in different geographic locations, but a lack of available data prevented us from incorporating such variation in our envelopes. Thus we assume a 45-day ripening period across varieties and regions, and tested the sensitivity of our results to this assumption (Figs. S20-S21). Then, for each 16,000 land pixels of the world we characterized the forecasted daily distribution of each climatic variable for each year within each warming period—e.g. 2°C, and 4°C—and our 0°C reference period. Finally, we classified each climatic variable as suitable or unsuitable for the target variety to reach maturity according to whether or not forecasted values for that variety fell within the 90% quantiles of the distribution. We set a 75% threshold for a given pixel to be classified as suitable, meaning that at least 6 out of the 8 climatic variables should have forecasted values within their distribution over our 30-year normal period. This approach is rather permissive—i.e. high quantile allowance and low threshold—in order to account for inter-year climatic variability and to reduce the amount of false negatives. Given the 30 ensemble members of our GCM we had a total of 300 estimates (300=30 GCM members x 10 years for each warming period) of climatic suitability for each pixel and each warming scenario.

Climatic suitability
See the main text *Materials & Methods* for how we calculated climatic suitability.

Our models of climatic suitability overlap significantly with current growing areas but exclude some areas; such areas may use unique practices to maintain vines, may use varieties very different than those we modelled (e.g., many areas in the southern and mid-west United States use hybrid vines that are not 100% *V. vinifera* subsp. *vinifera*), and/or may be areas our models suggested were suitable for winegrowing in too few years. Additionally, our estimates contain areas where winegrapes are not currently grown, including areas that have been highlighted in other studies of winegrowing areas (e.g., 17). We quantify gains and losses of climatic suitability for winegrowing by comparing the forecasted suitability under 2°C and 4°C with comparisons

to: (1) current growing regions and (2) areas our approach identified as climatically suitable under our 0°C reference period. Given that our models do not (and are not designed to) predict only areas currently growing winegrapes, estimates against current winegrowing areas could under or over-estimate changes. Thus, our two comparisons (current winegrowing regions and all climatically suitable regions under 0°C reference) capture both change relevant to current areas, and to our particular modeling approach.

Code availability and software used
Phenological parameterization and cross-validation was implemented with the software PMP v5.0 (61). All other analyses utilized custom computer R code, freely available at https://github.com/MoralesCastilla/ under the GNU General Public License.

Additional simulations & tests

Sensitivity analyses of indicators included in bioclimatic niche models
To test for the sensitivity of our results to including precipitation variables—e.g. Total summed precipitation, Maximum precipitation—in the maturation stage, we also modelled maturity based only on temperature variables (see above section on *Modeling maturity*): Growing Degree Days, Number of days above 40°C, Number of days below 10°C, Minimum daily temperatures, Maximum daily temperatures, Growing Degree Days above a threshold of 25°C. The ability of cultivar diversity to decrease the loss of climatically suitable regions holds when only temperature variables are accounted for to model maturity, regardless whether all potentially suitable regions (see Fig. S14b), or current growing regions of the world are considered (see Fig. S14d). Notably, by not accounting for precipitation variables in the models, the total amount of regions loss for any one single variety is higher, reaching 70% of average losses under the 2°C warming scenario (see Fig. S14d).

We also assessed whether our estimates of regions lost were sensitive to including minimum and maximum temperatures in our models. We found that our absolute estimates of regions lost were sensitive to these two variables being included—predicted losses are higher if minimum and maximum temperatures are considered (Fig. S14c)—however, our relative estimates were not: the overall pattern of cultivar diversity decreasing the loss of climatically suitable regions by almost a half was robust to whether these parameters were included in the model (Fig. S14).

Diurnal Temperature Range
Our bioclimatic niche models account for a wide array of indicators relevant for viticulture, but ignore additional potentially important indicators such as the daily variation in temperature. Shifts in Diurnal Temperature Range (DTR), mostly during the ripening phase, have been linked to major viticultural properties such as winegrape quality (62, 63), and berry development and chemical characteristics (64). Evidence for consistent directional shifts in DTR with climate warming is, however, scarce. Based in our future climate projections for a 2°C warming scenario (see above *Climate data*) we found that, shifts in DTR with 2°C of warming will not exceed 0.5°C locally and may affect the world's winegrowing regions unevenly—e.g. slight decreases in central Europe vs. mild increases in Southern Europe (Fig. S2). Future work on winegrape phenology may benefit from accounting for DTR in models and projections.

Although we do not include this variable in our bioclimatic niche models, we tested for the sensitivity of our results to dismissing DTR. Specifically, we re-ran our bioclimatic niche models for maturity of all 11 cultivars globally, adding DTR to our set of 8 bioclimatic indicators (see *Modelling maturity* above) and projected shifts under a +2°C warming scenario (results were averaged across five randomly selected simulations of the LENS model—i.e. simulations 5,7,14,19 and 26). Results show that DTR is less important for region loss than most other indicators, including precipitation variables (Fig. S18). Although low, the influence of DTR in determining climatic suitability appears important and should be considered in future studies, especially those at higher spatial resolutions or in regions known to be more influenced by DTR (e.g., 62).

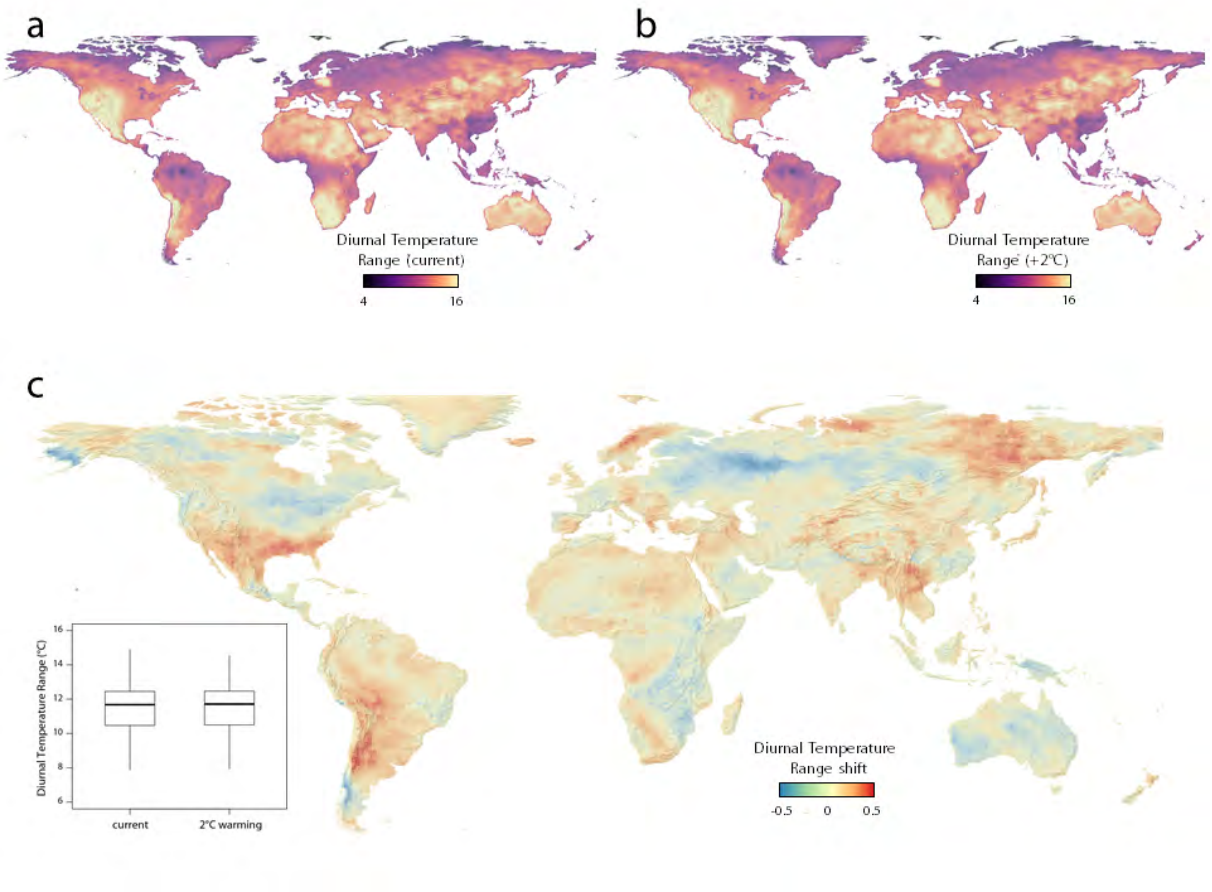

Fig. S2. Maps of Diurnal Temperature Range (DTR) measured globally for a 10-year period (2006-2015) representative of current climatic conditions (a), and the 10-year period (2039-2048) corresponding to the +2°C warming scenario (b). Shifts in DTR are calculated as the difference between current and projected DTR (c). The boxplot inset compares the distributions of DTR globally under both current and future climate, showing no significant differences in median DTR before and after warming. Across locations, however, recorded DTR shifts range between +0.5°C and -0.5°C with respect to current climatic conditions. These results are for one randomly selected GCM simulation of the LENS model.

Gains of climatic suitability

Our results identify a substantial impact of climate change in reducing the areas of both current winegrowing regions and other regions where wine is not cultivated but where climate would allow so. However, previous research (e.g., 17) has also highlighted that large extensions of territory may become suitable for winegrowing due to climate change. While gains of climatic suitability due to climate change are considerably lower than losses under both 2°C and 4°C warming scenarios (Fig. S14), these patterns are highly heterogeneous across geographic regions. For example, gains of climatic suitability were rather limited in Southern European countries like Spain, France or Italy (Fig. S15), and only occurred for varieties with later phenologies (e.g. Grenache, Monastrell or Ugni blanc, see Fig. S15). In contrast, gains of climatic suitability were highest in New World regions such as the Pacific Northwest (USA), New Zealand or California, not only for late varieties but also for earlier ones (e.g. Chardonnay, Riesling or Chasselas, see Fig. S15). Interestingly, gains of climatic suitability in the latter regions are highest under a 4°C warming scenario, but in European countries, most opportunities to gain climatic suitability coincide with the 2°C warming scenario. This information would be relevant for winegrowers from the regions with high potential to increase their suitability, by informing them of the varieties that may be best adapted to grow there in years to come.

Cultivar turnover also has a detectable effect on gains of climatic suitability (Fig. S19). The potential for gains of climatic suitability for any one variety is consistently higher under the 2°C than under the 4°C warming scenario (Fig. S19). Increasing diversity—i.e., allowing for cultivar turnover—from one to 11 varieties increases the amount of gains by 19.8% (i.e. from 80.2% of average gains when only one variety is considered to 100% gains when all are considered), under 2°C of warming (Fig. S19). A similar pattern, but showing a greater effect of turnover is found under 4°C of warming, with 43.1% increase in climatic suitability (i.e. from 56.9% of average gains when only one variety is consider to 100% gains when all are considered). These results thus show that our modeled varieties will have a larger potential to occupy novel growing regions under the 2°C scenario (i.e. climate suitability gains for winegrowing are greater under less warming), and also that the relative effects of cultivar turnover on suitability gains would be greater under 4°C of warming scenario.

Late-ripening composite (LRC) variety
To examine how including a much later-ripening cultivar impacts results, we parameterized and tested a hypothetical extremely late variety, built by combining our models with information on several late-ripening varieties. Our subset of 11 varieties captures significant phenological diversity (Fig. S4), but does not represent the full phenotypic variability existing within the genetic diversity of *Vitis vinifera* subsp. *vinifera*. In particular, our range of varieties fails to represent the later maturation exhibited by very late varieties (e.g. Nero amaro, Roditis or Maratheftiko). To include such phenotypic variability in our analyses, we simulated a virtual variety in an analogous way to previous approaches (65). To compute the parameters of this virtual variety, we find the maximum difference in C*, F*BB, F*Flo and F*Ver among the varieties included in our dataset, and either sum it or subtract it to the value of the variety with either maximum or minimum values for the parameters, respectively. Subsequently, for these set of parameters, we conducted all analyses, replicating the above described procedure for our 11 actual varieties.

The last step of our modeling workflow involves fitting bioclimatic envelopes to simulate maturity (see above), which requires data on the geographic distribution of each variety in order to estimate the climatic niche or the environmental space occupied by each variety over the 30-year normal period (1950-1980). Since we did not have distributional data for the hypothetical Late-ripening composite variety (LRC), we utilized as a surrogate the following varieties for which we had comprehensive enough distributional data, amongst those with the known later phenologies: Fogarina, Lambrusco Di Sorbara, Savatiano, Verdelho Tinto, Brun Argente, Amaral, Uva Cao and Verdicchio Bianco. Overall we selected 51 localities where these varieties are distributed, across Greece, Italy, France and Portugal (Fig. S3), that were later used to fit bioclimatic envelopes for the LRC variety.

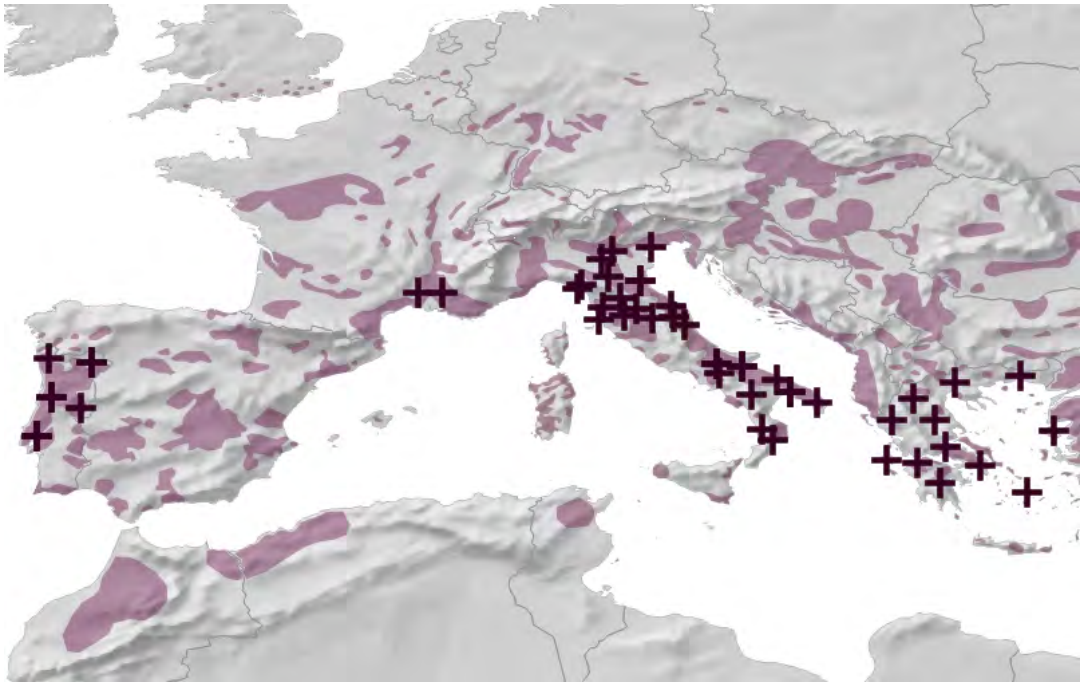

Fig. S3. Simulated geographical distribution of the Late-ripening composite (LRC) variety, based on the distribution of 8 varieties known to have late phenologies. The 51 points utilized to fit a bioclimatic envelope for the LRC variety are marked with crosses. In the background current winegrowing regions are shaded in purple.

Overall, including the LRC has an almost negligible effect on our results. Analyses of loss of climatic suitability within current winegrowing regions revealed that including the LRC decreased region loss by less than 1% (Fig. S14): under 2°C of warming, 23.6% out of all global current winegrowing regions would lose their climatic suitability for winegrowing even after including our simulated LRC. This figure does not represent a large improvement in comparison with the 24% that would be loss allowing for turnover across the 11 varieties in our study. This result supports that cultivar diversity can buffer loss of agricultural regions but such ability is not unlimited. However, modeling one virtual variety is a suboptimal option in comparison to modeling one (or several) actual late-ripening variety (e.g. Maratheftiko), which may potentially have a tolerance to high temperatures. Unfortunately, modeling further late-ripening varieties was unfeasible due to data limitations and thus, future work will benefit from systematic collection of phenological data for less-known, Southern European varieties.

Sensitivity analyses based on veraison-harvest temporal window
Our models for maturity (see above section on *Modeling maturity*) assumed for all varieties a temporal window of 45 days following veraison within which climatic variables were recorded to build the climatic envelopes. A 45-day period for winegrapes to ripen is empirically supported for most varieties, however, certain varieties have ripening periods shorter or longer than 45

days in some sites and years (25, 66). To provide some assessment of the effect that our choice of a 45-day veraison-harvest period would have on estimates for gains and losses of winegrowing regions we re-fitted climatic envelopes for *Chasselas*, the variety with the shortest veraison-harvest period in our dataset.

We first evaluated shifts in the distribution of the values of each climatic variable according to a 30-day period after veraison against a 45-day period (Fig. S20). Results show an overall close match among the climatic distributions of each variable regardless of whether the distribution is recorded over the 30 or the 45 days following the predicted veraison date. An exception to this pattern was found for Summed precipitation and Growing Degree Days, which is expected given that more precipitation and more Degree Days can accumulate in 45 than in 30 days.

In a second step we replicated our analyses quantifying climatic suitability to reach maturity for Chasselas within Europe based on the 30 days following veraison instead of the 45-day window employed in our main analyses. Climatic suitability was calculated under the same three scenarios that were used to estimate increases and decreases in suitable regions (by comparing the amount of climatically suitable regions at 0°C, with suitable regions at both 2°C and 4°C of warming). Results showed similar trends, but magnified estimates of both gains and losses of suitable regions (Fig. S21). Thus, if climatic envelopes were characterized across a shorter period, the proportion of climatic suitability loss would increase —e.g. from 71.2% to 81.9% on average under 2°C warming—and the proportion of current growing regions becoming more suitable to grow Chasselas would decrease—e.g. from 15% to 0.2% on average under 2°C warming— S21. These results confirm that our approach is conservative in estimating both losses and gains.

References

1. Coombe BG, Dry PR (1992) *Viticulture, Volume 2: Practices.* (Winetitles, Adelaide, South Australia).
2. Parker AK, García De Cortázar-Atauri I, van Leeuwen C, Chuine I (2011) General phenological model to characterise the timing of flowering and veraison of *Vitis vinifera* L. *Australian Journal of Grape and Wine Research* 17(2):206–216.
3. Anderson K, Aryal NR (2015) *Which winegrape varieties are grown where? A global empirical picture.* (University of Adelaide Press).
4. Robinson J, Harding J (2015) *The Oxford Companion to Wine.* (Oxford University Press, New York), 4th edition.
5. Bock A, Sparks T, Estrella N, Menzel A (2011) Changes in the phenology and composition of wine from Franconia, Germany. *Climate Research* 50(1):69–81.
6. Malheiro AC, et al. (2013) Winegrape phenology and temperature relationships in the Lisbon wine region, Portugal. *Journal International Des Sciences De La Vigne Et Du Vin* 47(4):287–299.
7. Ruml M, Korac N, Vujadinovic M, Vukovic A, Ivanisevic D (2016) Response of grapevine phenology to recent temperature change and variability in the wine-producing area of Sremski Karlovci, Serbia. *Journal of Agricultural Science* 154(2):186–206.
8. Cayan D, Nicholas KA, Tyree M, Dettinger M (2011) Climate and phenology in Napa Valley: A compilation and analysis of dhistorical data. Private report to the Napa Valley Vintners., Executive summary report.
9. Wolkovich EM, Burge DO, Walker MA, Nicholas KA (2017) Phenological diversity provides opportunities for climate change adaptation in winegrapes. *Journal of Ecology* 105(4):905–912.
10. Boursiquot JM, Dessup M, Rennes C (1995) Distribution des principaux caractères phénologiques, agronomiques et technologiques chez *Vitis vinifera* L. *Vitis* 34(1):31–35.
11. Clarke O (2007) *Oz Clarke Wine Atlas: Wines and Wine Regions of the World.* (Anova Books).
12. Morales-Castilla I, Fernández-Pastor M, Wolkovich EM (2019) Winegrowing regions of the world 2007. *Knowledge Network for Biocomplexity.*
13. Kay JE, et al. (2015) The Community Earth System Model (CESM) Large Ensemble Project A community resource for studying climate change in the presence of internal climate variability. *Bulletin of the American Meteorological Society* 96(8):1333–1349.
14. Fraga H, Malheiro AC, Moutinho-Pereira J, Santos JA (2013) Future scenarios for viticultural zoning in europe: ensemble projections and uncertainties. *International Journal of Biometeorology* 57(6):909–925.
15. Moriondo M, et al. (2013) Projected shifts of wine regions in response to climate change. *Climatic Change* 119(3-4):825–839.
16. Cuccia C, et al. (2014) Phenological model performance to warmer conditions: application to Pinot noir in Burgundy. *J Int Sci Vigne Vin* 48(3):169–78.
17. Hannah L, et al. (2013) Climate change, wine, and conservation. *Proceedings of the National Academy of Sciences* 110(17):6907–6912.
18. Mills LJ, Ferguson JC, Keller M (2006) Cold-hardiness evaluation of grapevine buds and cane tissues. *American Journal of Enology and Viticulture* 57(2):194–200.
19. Davenport JR, Keller M, Mills LJ (2008) How cold can you go? Frost and winter protection for grape. *HortScience* 43(7):1966–1969.
20. Richardson E (1974) A model for estimating the completion of rest for 'Redhaven' and 'Elberta' peach trees. *HortScience* 9:331–332.
21. Bonhomme M, Rageau R, Lacointe A (2010) Optimization of endodormancy release models, using series of endodormancy

release data collected in france in *VIII International Symposium on Temperate Zone Fruits in the Tropics and Subtropics 872*. pp. 51–60.
22. Wang E, Engel T (1998) Simulation of phenological development of wheat crops. *Agricultural Systems* 58(1):1–24.
23. García de Cortázar-Atauri I, Chuine I, Donatelli M, Parker A, van Leeuwen C (2010) A curvilinear process-based phenological model to study impacts of climatic change on grapevine (*Vitis vinifera* L.). *Proceedings of Agro* pp. 907–908.
24. Parent B, Tardieu F (2012) Temperature responses of developmental processes have not been affected by breeding in different ecological areas for 17 crop species. *New Phytologist* 194(3):760–774.
25. García de Cortázar-Atauri I, et al. (2010) Climate reconstructions from grape harvest dates: Methodology and uncertainties. *Holocene* 20(4):599–608.
26. Champagnol F (1984) *Éléments de physiologie de la vigne et de viticulture générale*. (Saint-Gely-du-Fesc, France).
27. Jones GV (2013) Winegrape Phenology in *Phenology: An Integrative Environmental Science*, ed. Schwartz MD. (Springer, Dordrecht, the Netherlands), pp. 563–584.
28. Zaka S, et al. (2017) How variable are non-linear developmental responses to temperature in two perennial forage species? *Agricultural and Forest Meteorology* 232:433–442.
29. Alleweldt G, Eibach R, Ruhl E (1982) Investigations on gas exchange in grapevine [vitis], pt. 1: Influence of temperature, leaf age and daytime on net photosynthesis and transpiration. *Vitis* 21:93–100.
30. Zufferey V, Murisier F, Schultz H, , et al. (2000) A model analysis of the photosynthetic response of *Vitis vinifera* L. cvs Riesling and Chasselas leaves in the field: I. Interaction of age, light and temperature. *Vitis* 39(1):19–26.
31. Kriedemann P (1968) Photosynthesis in vine leaves as a function of light intensity, temperature, and leaf age.
32. Kriedemann P, Smart R (1971) Effects of irradiance, temperature, and leaf water potential on photosynthesis of vine leaves.
33. Huglin P, Schneider C (1998) Biologie et écologie de la vigne [biology and ecology of the vineyard]. *Paris: Ed. Lavoisier Tec & Doc*.
34. Janssen P, Heuberger P (1995) Calibration of process-oriented models. *Ecological Modelling* 83(1-2):55–66.
35. Wallach D (2006) *Evaluating crop models*, eds. Wallach D, Makowski D, Jones JW. (Elsevier, Amsterdam), pp. 6–37.
36. Chuine I, et al. (2016) Can phenological models predict tree phenology accurately in the future? the unrevealed hurdle of endodormancy break. *Global Change Biology* 22(10):3444–3460.
37. Nash JE, Sutcliffe JV (1970) River flow forecasting through conceptual models part i — a discussion of principles. *Journal of Hydrology* 10(3):282–290.
38. Luedeling E (2013) ChillR: statistical methods for phenology analysis in temperate fruit trees. R package version 0.54.
39. García de Cortázar-Atauri I, Brisson N, Ollat N, Jacquet O, Payan JC (2009) Asynchronous dynamics of grapevine ("Vitis vinifera") maturation: experimental study for a modelling approach. *OENO One* 43(2):83–97.
40. Chuine I, Cour P, Rousseau D (1999) Selecting models to predict the timing of flowering of temperate trees: implications for tree phenology modelling. *Plant, Cell & Environment* 22(1):1–13.
41. Hänninen H, , et al. (1990) Modelling bud dormancy release in trees from cool and temperate regions.
42. Wang E, et al. (2017) The uncertainty of crop yield projections is reduced by improved temperature response functions. *Nature Plants* 3:17102 EP –.
43. Fila G, Gardiman M, Belvini P, Meggio F, Pitacco A (2014) A comparison of different modelling solutions for studying grapevine phenology under present and future climate scenarios. *Agricultural and Forest Meteorology* 195:192–205.
44. Parker AK, Hofmann RW, van Leeuwen C, McLachlan AR, Trought MC (2014) Leaf area to fruit mass ratio determines the time of veraison in Sauvignon Blanc and Pinot Noir grapevines. *Australian Journal of Grape and Wine Research* 20(3):422–431.
45. Costa R, et al. (2019) Grapevine Phenology of cv. Touriga Franca and Touriga Nacional in the Douro Wine Region: Modelling and Climate Change Projections. *Agronomy* 9(4):210.
46. Webb L, et al. (2012) Earlier wine-grape ripening driven by climatic warming and drying and management practices. *Nature Climate Change* 2(4):259.
47. Torregrosa L, et al. (2017) Developmental, molecular and genetic studies on grapevine response to temperature open breeding strategies for adaptation to warming. *Oeno* One 51(2):155–165.
48. Rienth M, et al. (2016) Temperature desynchronizes sugar and organic acid metabolism in ripening grapevine fruits and remodels their transcriptome. *Bmc Plant Biology* 16.
49. García de Cortázar-Atauri I, et al. (2017) Grapevine phenology in france: from past observations to future evolutions in the context of climate change. *OENO One* 51(2).
50. van Leeuwen C, et al. (2009) Vine water status is a key factor in grape ripening and vintage quality for red bordeaux wine. how can it be assessed for vineyard management purposes. *J. Int. Sci. Vigne Vin* 43(3):121–134.
51. Pearson RG, Dawson TP (2003) Predicting the impacts of climate change on the distribution of species: are bioclimate envelope models useful? *Global Ecology and Biogeography* 12(5):361–371.
52. Araújo MB, Peterson AT (2012) Uses and misuses of bioclimatic envelope modeling. *Ecology* 93(7):1527–1539.
53. Huglin P (1978) Nouveau mode d'évaluation des possibilités héliothermiques d'un milieu viticole. *Comptes rendus des seances*.
54. Winkler A, Cook J, Kliewer W, Lider L (1974) Means of improving grape quality. *General Viticulture* 710.
55. Tonietto J, Carbonneau A (2004) A multicriteria climatic classification system for grape-growing regions worldwide.

Agricultural and Forest Meteorology 124(1-2):81–97.
56. Coombe B (1986) Influence of temperature on composition and quality of grapes. Vol. 206, pp. 23–36.
57. Pons A, Allamy L, Lavigne V, Dubourdieu D, Darriet P (2017) Study of the contribution of massoia lactone to the aroma of merlot and cabernet sauvignon musts and wines. *Food Chemistry* 232:229–236.
58. Happ E (1999) Indices for exploring the relationship between temperature and grape and wine flavour. *Australian and New Zealand Wine Industry Journal* 14:68–76.
59. Ben-Ari T, et al. (2018) Causes and implications of the unforeseen 2016 extreme yield loss in the breadbasket of france. *Nature Communications* 9(1):1627.
60. Allouche O, Tsoar A, Kadmon R (2006) Assessing the accuracy of species distribution models: prevalence, kappa and the true skill statistic (tss). *Journal of Applied Ecology* 43(6):1223–1232.
61. Chuine I, García de Cortázar-Atauri I, Kramer K, Hänninen H (2013) Plant development models in *Phenology: an integrative environmental science*. (Springer), pp. 275–293.
62. White MA, Diffenbaugh N, Jones GV, Pal J, Giorgi F (2006) Extreme heat reduces and shifts united states premium wine production in the 21st century. *Proceedings of the National Academy of Sciences* 103(30):11217–11222.
63. Davis RE, Dimon RA, Jones GV, Bois B (2019) The effect of climate on Burgundy vintage quality rankings. *OENO One* 53(1).
64. Cohen SD, Tarara JM, Gambetta GA, Matthews MA, Kennedy JA (2012) Impact of diurnal temperature variation on grape berry development, proanthocyanidin accumulation, and the expression of flavonoid pathway genes. *Journal of experimental botany* 63(7):2655–2665.
65. Duchêne E, Huard F, Dumas V, Schneider C, Merdinoglu D (2010) The challenge of adapting grapevine varieties to climate change. *Climate Research* 41(3):193–204.
66. Yiou P, et al. (2012) Continental atmospheric circulation over Europe during the Little Ice Age inferred from grape harvest dates. *Climate of the Past* 8(2):577–588.
67. Seguin B (2004) The phenoclim database for fruit trees and vine in france. *Challenging Times* p. 75.
68. Adelsheim D, et al. (2016) Climate change: Field reports from leading winemakers. *Journal of Wine Economics* 11(1):5–47.

Tables

Table S1. Summary of data used to parameterize phenological models. For each site for which we had data, we indicate its geographic coordinates, the minimum and maximum year of observation, the phenological stage (BB for budbreak, FL for flowering, VER for verasison) for which there was data (marked with x), and the winegrape varieties observed. Part of these data are from Phenoclim Database (INRA Vassal, Colmar, Angers, Bordeaux, Pech Rouge - https://www6.inra.fr/soere-tempo/Ressources/Portail-de-donnees) - Seguin (2004).

Site	Lon	Lat	Years	minYear	maxYear	BB	FL	VER	Varieties
1	4.58	48.05	4	1999	2002	x	x	x	Chardonnay, Pinot noir
2	5.14	43.55	1	2003	2003	x	x	x	Syrah
3	5.67	43.52	2	2006	2007	x	x	x	Grenache
4	5.43	43.66	1	2006	2006	x	x	x	Grenache
5	5.55	43.73	3	2005	2007	x	x	x	Grenache
6	2.65	43.18	3	2000	2002	x	x	x	Monastrell
7	4.99	47.27	2	2004	2005	x	x	x	Chardonnay, Pinot noir
8	4.41	43.78	2	2004	2005	x	x	x	Grenache, Syrah
9	4.56	44.30	5	1999	2003	x	x	x	Monastrell
10	4.49	44.14	2	2001	2003	x	x	x	Monastrell
11	4.68	43.94	4	1999	2003	x	x	x	Monastrell
12	4.70	44.01	4	1999	2003	x	x	x	Monastrell
13	4.56	43.88	5	1999	2003	x	x	x	Monastrell
14	4.43	43.80	5	1999	2003	x	x	x	Monastrell
15	-0.47	44.77	28	1974	2001	x	x	x	Merlot, Cabernet-Sauvignon
16	-0.56	44.75	1	2004	2004	x	x	x	Merlot
17	-0.16	44.89	4	2000	2003	x	x	x	Merlot
18	-0.20	44.93	3	2001	2003	x	x	x	Merlot
19	-0.19	44.92	12	1995	2006	x	x	x	Merlot, Cabernet-Sauvignon
20	-0.77	45.21	15	1990	2004	x	x	x	Sauvignon blanc
21	3.56	43.33	50	1956	2005	x	x	x	Chasselas, Monastrell, Riesling, Pinot noir, Chardonnay, Grenache, Sauvignon blanc, Syrah, Ugni blanc, Cabernet-Sauvignon , Tempranillo, Merlot
22	3.92	43.84	2	2004	2005	x	x	x	Grenache, Syrah
23	3.17	43.27	3	1997	1999	x	x	x	Cabernet-Sauvignon
24	3.17	43.61	1	2005	2005	x	x	x	Chardonnay, Syrah
25	3.32	43.34	3	1997	2006	x	x	x	Riesling, Chardonnay
26	3.10	43.58	1	2005	2005	x	x	x	Chardonnay, Syrah
27	2.91	43.56	1	2005	2005	x	x	x	Chardonnay, Syrah
28	3.42	43.46	8	1999	2006	x	x	x	Merlot, Monastrell, Chardonnay, Riesling
29	3.14	43.44	2	2003	2004	x	x	x	Grenache
30	3.28	43.48	6	2001	2006	x	x	x	Syrah, Merlot
31	3.04	43.37	5	2002	2006	x	x	x	Merlot, Syrah
32	3.20	43.52	1	2003	2003	x	x	x	Monastrell
33	3.03	43.50	1	2002	2002	x	x	x	Monastrell
34	3.87	43.80	3	2003	2005	x	x	x	Syrah
35	-0.16	47.13	22	1981	2005	x	x	x	Chasselas, Riesling, Grenache, Sauvignon blanc, Syrah, Ugni blanc, Cabernet-Sauvignon
36	3.95	49.05	7	1998	2004	x	x	x	Chardonnay, Pinot noir
37	3.98	49.02	6	1999	2004	x	x	x	Chardonnay, Pinot noir
38	7.36	48.20	40	1976	2015	x	x	x	Cabernet-Sauvignon , Chardonnay, Chasselas, Merlot, Pinot noir, Riesling, Syrah, Ugni blanc, Grenache, Sauvignon blanc
39	6.23	43.14	4	2002	2007	x	x	x	Grenache
40	6.07	43.24	1	1999	1999	x	x	x	Monastrell
41	6.53	43.25	3	2005	2007	x	x	x	Grenache
42	6.12	43.47	3	2005	2007	x	x	x	Grenache
43	5.78	43.20	1	2007	2007	x	x	x	Grenache
44	4.76	44.18	1	2004	2004	x	x	x	Grenache, Syrah
45	4.94	43.93	8	1997	2004	x	x	x	Grenache, Syrah
46	5.13	44.27	4	2000	2003	x	x	x	Grenache
47	5.06	44.08	8	1998	2005	x	x	x	Grenache, Syrah
48	4.96	44.16	4	1999	2002	x	x	x	Monastrell
49	4.80	44.21	4	2000	2003	x	x	x	Monastrell
50	5.07	44.17	4	1999	2002	x	x	x	Monastrell
51	5.24	43.86	4	2000	2003	x	x	x	Monastrell
52	5.06	43.86	4	1999	2003	x	x	x	Monastrell
53	4.81	44.08	4	1999	2003	x	x	x	Monastrell
54	4.93	44.23	3	1999	2001	x	x	x	Monastrell
55	4.93	44.23	2	2000	2002	x	x	x	Monastrell
56	5.05	44.09	2	2006	2007	x	x	x	Grenache
57	4.83	44.06	3	2005	2007	x	x	x	Syrah, Grenache
58	5.15	43.89	1	2006	2006	x	x	x	Grenache
59	4.93	43.96	3	2005	2007	x	x	x	Grenache, Syrah
60	5.18	44.12	3	2005	2007	x	x	x	Grenache, Syrah
61	5.05	43.80	2	2006	2007	x	x	x	Grenache
62	7.97	49.98	40	1974	2013	x	x	x	Pinot noir

Table S2. Summary of European and North American sources used to validate phenological models with independent observational data. For each site, we indicate its geographic coordinates, the minimum and maximum year of observation, the phenological stage for which there was data (marked with x), and the winegrape varieties observed. Data for European locations comes from published work (i.e. Bock et al. (2013); Malheiro et al. (2013); Ruml et al. (2015)) and reports means and standard deviations of the observations. Data for North American locations comes from a data report (Cayan et al. (2010) for Napa Valley) and own-collected data (Wolkovich et al. 2017), and includes raw observations of yearly timing of each phenological stage (i.e. BB for budbreak, FL for flowering, VER for veraison) for each variety.

Site.ID	Lon	Lat	Years	minYear	maxYear	BB	FL	VER	Varieties
Bock	9.87	49.83	38	1968	2010	x	x	x	Riesling
Malheiro	-9.20	39.00	22	1990	2011	x	x	x	Chasselas
Ruml	20.17	45.17	25	1986	2011	x	x	x	Cabernet Sauvignon, Pinot noir, Merlot, Chardonnay, Riesling
Napa	-122.29	38.30	19	1985	2007	x	x	x	Cabernet Sauvignon, Merlot, Chardonnay, Sauvignon blanc
Davis	-121.74	38.54	4	2013	2016	x	x	x	Cabernet Sauvignon, Chardonnay, Chasselas, Merlot, Monastrell, Pinot noir, Riesling, Sauvignon blanc, Syrah, Ugni blanc

Table S3. Comparison of combined dormancy-post-dormancy models for budbreak. Compared alternatives include the Smoothed-Utah (Richardson 1974), BRIN (García de Cortázar-Atauri et al 2009) and Chuine (Chuine et al. 1999) models for dormancy and the Richardson (Richardson 1974), sigmoid (Hanninen et al. 1990) and Wang-Engel (Wang & Engel 1998) models for the post-dormancy phase. Model accuracy was calculated through the Root Mean Square Error (RMSE), the Efficiency (EF) and the Akaike Information Criterion (AIC; Anderson et al. 1994). The number of fitted parameters is shown for the dormancy (Dorm.) and Post-dormancy (Post-dorm.).

Model	n	Dorm.	Post-dorm.	RMSE	EF	AIC
BRIN + Richardson	482	2	1	7.58	0.74	1958.70
Smoothed-Utah + Richardson	482	5	1	7.40	0.76	1941.21
Smoothed-Utah + Wang-Engel	482	5	2	7.19	0.77	1916.25
Smoothed-Utah + Sigmoid	482	5	3	7.16	0.77	1914.30
Chuine + Richardson	482	4	1	7.50	0.75	1953.03
Chuine + Richardson (free parameter)	482	4	3	7.44	0.75	1948.44
Chuine + Sigmoid	482	4	3	7.29	0.76	1929.01
Chuine + Wang-Engel	482	4	2	7.41	0.75	1943.16

Table S4. Parameterization of winegrapes to sequential phenological models from dormancy to budbreak (Smoothed-Utah model, SU), to flowering and veraison (Wang and Engel, WE). The SU model includes four parameters: 1) Tm1 or decrease in cold efficiency for bud endodormancy, 2) Topt optimal mean daily temperature, 3) Tn2 the temperature with half the efficiency of Topt to induce endodormancy, and 4) min the negative impact of high temperatures. The WE model includes three parameters: 1) Tmin, 2) Topt.1, and 3) Tmax, representing the minimum, optimum and maximum temperature values to calculate the amount of forcing, respectively (for details see Methods section above). The units for all parameters are in °C. Fitted parameters are identical across varieties.

SU.params	SU.values	WE.params	BB.values	BB.FL.values	FL.VER.values
Tm1	-6.70	Tmin	0	0	0
Topt	7.94	Topt.1	26.1	29.34	21.84
Tn2	40.58	Tmax	40	40	40
min	-0.17				

Table S5. Chilling (C*) and forcing (F*) parameters, used as thresholds above which a given phenological stage from dormancy to budbreak (C* BB and F* BB), from budbreak to flowering (F* BB-FL) and from flowering to veraison (F* FL-VER) is reached. The units are in number of days for all parameters.

Variety	C* BB	F* BB	F* BB-FL	F* FL-VER
Cabernet-Sauvignon	166.02	20.24	23.61	65.30
Chardonnay	199.01	12.50	22.26	63.28
Chasselas	196.68	12.40	24.46	53.40
Grenache	197.68	14.02	24.71	66.90
Merlot	152.14	19.91	24.96	64.45
Monastrell	216.56	7.64	28.04	62.07
Pinot noir	198.53	12.98	21.85	59.50
Riesling	185.38	14.08	22.13	64.63
Sauvignon blanc	203.48	13.06	25.34	59.27
Syrah	198.63	13.55	23.91	59.99
Ugni blanc	199.74	17.80	24.41	67.36
Late-ripening composite	232.67	23.39	29.59	70.85

Table S6. Comparison between the parameterization of winegrapes in Table S4, based on gridded climate data extracted from BEST (Berkley Earth Surface Temperatures) and a parameterization resulting from using local weather station data. As in Table S4 the models cover sequential phenological stages from dormancy to budbreak (Smoothed-Utah model, SU), to flowering and veraison (Wang and Engel, WE). Note that fitted parameters are identical across varieties. The units for all parameters are °C. Note that the Tmin and Tmax parameters were fixed at 0 and 40°C, respectively, for both climatic datasets. Values of Tmax of 40°C were selected after comparison against alternative values (e.g. 36, 37, 38, 39°C).

SU.params	SU.values	WE.params	BB.values	BB.FL.values	FL.VER.values
Tm1 local weather	-10.83	Tmin local weather	0	0	0
Topt local weather	11.13	Topt.1 local weather	28	30.92	25.08
Tn2 local weather	29.67	Tmax local weather	40	40	40
min local weather	-0.32				
Tm1 BEST data	-6.70	Tmin BEST data	0	0	0
Topt BEST data	7.94	Topt.1 BEST data	26.1	29.34	21.84
Tn2 BEST data	40.58	Tmax BEST data	40	40	40
min BEST data	-0.17				

Table S7. Comparison between the parameterization of winegrapes in Table S5, based on gridded climate data extracted from BEST (Berkley Earth Surface Temperatures; http://berkeleyearth.org/data/) and a parameterization resulting from using local weather station data. As in Table S5 the (C*) and forcing (F*) parameters, used as thresholds above which a given phenological stage from dormancy to budbreak (C* BB and F* BB), from budbreak to flowering (F* BB-FL) and from flowering to veraison (F* FL-VER) is reached. The phenological stages parameterized are BB (budbreak), FL (flowering) and VER (veraison). The units for all parameters are the number of days.

Variety	C* BB	F* BB	F* BB-FL	F* FL-VER
Cabernet-Sauvignon Weather data	158.34	16.09	16.56	60.84
Cabernet-Sauvignon BEST data	166.02	20.24	23.61	65.30
Chardonnay Weather data	189.44	9.86	15.35	58.98
Chardonnay BEST data	199.01	12.50	22.26	63.28
Chasselas Weather data	193.20	10.14	17.24	49.53
Chasselas BEST data	196.68	12.40	24.46	53.40
Grenache Weather data	187.40	11.44	17.49	63.98
Grenache BEST data	197.68	14.02	24.71	66.90
Merlot Weather data	144.72	16.16	17.28	60.35
Merlot BEST data	152.14	19.91	24.96	64.45
Monastrell Weather data	171.13	15.42	20.34	60.43
Monastrell BEST data	216.56	7.64	28.04	62.07
Pinot noir Weather data	194.18	10.27	15.29	54.53
Pinot noir BEST data	198.53	12.98	21.85	59.50
Riesling Weather data	190.22	10.32	15.50	59.88
Riesling BEST data	185.38	14.08	22.13	64.63
Sauvignon blanc Weather data	192.22	10.26	17.76	55.16
Sauvignon blanc BEST data	203.48	13.06	25.34	59.27
Syrah Weather data	191.43	11.05	16.88	57.19
Syrah BEST data	198.63	13.55	23.91	59.99
Ugni blanc Weather data	216.88	10.18	17.23	62.47
Ugni blanc BEST data	199.74	17.80	24.41	67.36

Table S8. Validation of phenological modeling results against independent observations of winegrape phenology corresponding to dates of budbreak (BB), flowering (FL) and veraison (VER). Independent observations are extracted from Bock et al. (2011), Malheiro et al. (2013) and Ruml et al. (2015) in Europe, where only means and standard deviations of observations are provided. And from Cayan et al. (2010) in North America, where full yearly observations of each phenophase were available. Results are for Riesling (Rsl), Chasselas (Chs), Pinot noir (Pn), Cabernet-Sauvignon (C-S), Merlot (Mrl), Chardonnay (Chr) and Sauvignon blanc (S-b). Model predictions and observations from Bock et al. (2011) and Malheiro et al. (2013) for flowering and veraison were for when 50% of clusters were at stages BBCH 65 and 81, respectively (these correspond to modified Eichorn-Lorenz of 23 and 35); for Ruml et al. (2015), observations are for the beginning of these stages (while our model estimates are for the mid-point—thus our model would not be expected to accurately predict these observations). Budburst is defined as green shoot tips visible for all observations and model predictions. Values shown correspond to averages and associated confidence intervals (95%) across observations and model predictions over the period for which phenological data were available. RPD and RMSE values could be computed only for Napa, as it was the only dataset where yearly observations matched yearly predictions. For European data validation is restricted to comparison of means of observed and predicted values. Note that data from Davis in Wolkovich et al. (2017) was not evaluated here due to lack of long enough temporal resolution—i.e. 4 years of observations—but see Fig. S6.

Dataset	Phenophase	Observed	Predicted	RPD	RMSE
Bock (Rsl)	BB	122.00 ± 10.00	118.57 ± 16.50		
Bock (Rsl)	FL	175.00 ± 9.00	177.10 ± 16.20		
Bock (Rsl)	VER	236.00 ± 12.00	246.62 ± 18.20		
Malheiro (Chs)	BB	73.00 ± 8.00	80.25 ± 7.20		
Malheiro (Chs)	FL	140.00 ± 9.00	139.50 ± 13.20		
Malheiro (Chs)	VER	208.00 ± 11.00	195.06 ± 13.30		
Ruml (Pn)	BB	99.00 ± 10.50	108.07 ± 14.50		
Ruml (Pn)	FL	148.00 ± 7.80	158.20 ± 11.50		
Ruml (Pn)	VER	203.00 ± 9.70	219.87 ± 11.00		
Ruml (C-S)	BB	108.00 ± 6.70	114.67 ± 17.00		
Ruml (C-S)	FL	151.00 ± 7.60	164.20 ± 11.90		
Ruml (C-S)	VER	212.00 ± 8.50	231.83 ± 12.10		
Ruml (Mrl)	BB	104.00 ± 8.30	112.52 ± 19.70		
Ruml (Mrl)	FL	149.00 ± 8.10	165.50 ± 12.70		
Ruml (Mrl)	VER	212.00 ± 10.50	232.16 ± 12.90		
Ruml (Chr)	BB	97.00 ± 10.70	107.24 ± 14.80		
Ruml (Chr)	FL	146.00 ± 8.30	158.50 ± 11.30		
Ruml (Chr)	VER	205.00 ± 8.90	224.08 ± 10.90		
Ruml (Rsl)	BB	102.00 ± 9.30	106.18 ± 16.00		
Ruml (Rsl)	FL	149.00 ± 7.40	157.74 ± 12.20		
Ruml (Rsl)	VER	211.00 ± 10.20	224.86 ± 11.80		
Napa (C-S)	BB	90.27 ± 13.58	84.69 ± 15.91	1.06	2.26
Napa (C-S)	FL	143.86 ± 15.27	150.29 ± 15.23	0.97	2.37
Napa (C-S)	VER	214.66 ± 17.14	218.03 ± 15.61	1.68	1.4
Napa (Chr)	BB	81.16 ± 12.96	87.99 ± 13.27	0.72	2.54
Napa (Chr)	FL	135.85 ± 21.62	148.82 ± 15.32	0.43	4.9
Napa (Chr)	VER	208.51 ± 25.10	214.65 ± 15.63	0.69	3.02
Napa (Mrl)	BB	87.35 ± 16.62	76.24 ± 14.96	0.67	2.78
Napa (Mrl)	FL	143.27 ± 19.36	149.28 ± 15.25	0.95	2
Napa (Mrl)	VER	218.77 ± 19.52	216.20 ± 15.20	2.36	0.8
Napa (S-b)	BB	86.86 ± 13.13	92.33 ± 13.34	0.82	2.08
Napa (S-b)	FL	145.40 ± 16.71	157.16 ± 14.69	0.55	3.43
Napa (S-b)	VER	208.72 ± 18.63	218.42 ± 14.89	0.63	3.01

Table S9. Results of uncertainty, accuracy and cross-validation relative to calibrated parameters. Uncertainty around fitted parameters is measured as lower and upper 95% Confidence Intervals (CI). Accuracy of each calibration is shown by the RMSE and EF metrics. Cross-validation results following a leave-one-out procedure (analogous to that in Chuine et al. 2016) are shown by RMSEP. EF, RMSE and RMSEP are defined above in 'Phenological Modeling' section. Values for C* and F* are in the chilling and forcing units, respectively, necessary for a phenological event to occur. The units of threshold parameters (C*, F*) and RMSE and RMSEP are in days. RPD is included for parameters obtained with BEST to allow comparability with other validation results. Abbreviations are used for Cabernet Sauvignon (C-S), Chardonnay (Chr), Chasselas (Chs), Grenache (Gre), Merlot (Mrl), Monastrell (Mon), Pinot noir (P-n), Riesling (Rsl), Sauvignon blanc (S-b) and Ugni blanc (U-b). Weather or BEST indicate what climatic data was used to parameterize the data and BB, FL and VER indicate the phenological stage of budbreak, flowering and veraison, respectively.

Variety_Data_Stage	C*	C* CI.low	C* CI.up	F*	F* CI.low	F* CI.up	RMSE	EF	RMSEP	RPD
C-S_BEST_BB	166.02	157.91	180.47	20.24	17.86	21.50	5.70	0.91	6.38	3.35
C-S_BEST_FL				23.61	22.64	24.62	4.60	0.90	4.73	3.12
C-S_BEST_VER				65.30	63.95	66.62	5.36	0.86	5.44	2.36
C-S_Weather_BB	158.34	149.33	166.34	16.09	14.79	16.95	5.96	0.90	7.42	
C-S_Weather_FL				16.56	15.88	17.26	4.51	0.90	4.70	
C-S_Weather_VER				60.84	59.60	62.01	5.24	0.86	5.31	
Chr_BEST_BB	199.01	192.02	203.51	12.50	11.59	13.73	7.92	0.53	8.21	1.46
Chr_BEST_FL				22.26	21.55	22.95	4.05	0.85	4.19	2.61
Chr_BEST_VER				63.28	61.30	65.35	7.46	0.82	7.60	2.37
Chr_Weather_BB	189.44	187.17	195.42	9.86	9.26	10.22	6.85	0.65	7.53	
Chr_Weather_FL				15.35	14.90	15.82	3.78	0.87	3.90	
Chr_Weather_VER				58.98	57.45	60.50	5.92	0.89	6.07	
Chs_BEST_BB	196.68	192.24	205.71	12.40	11.14	14.11	6.15	0.55	7.72	1.49
Chs_BEST_FL				24.46	23.74	25.22	3.62	0.86	3.72	2.68
Chs_BEST_VER				53.40	52.07	54.77	5.12	0.92	5.21	3.44
Chs_Weather_BB	193.20	189.64	195.10	10.14	9.76	10.59	5.02	0.70	5.35	
Chs_Weather_FL				17.24	16.77	17.72	3.19	0.89	3.28	
Chs_Weather_VER				49.53	48.47	50.55	4.25	0.94	4.32	
Gre_BEST_BB	197.68	195.36	205.78	14.02	12.45	14.67	7.21	0.79	8.00	2.18
Gre_BEST_FL				24.71	24.18	25.34	3.64	0.94	3.71	4.21
Gre_BEST_VER				66.90	65.20	68.52	7.77	0.81	7.88	2.29
Gre_Weather_BB	187.40	162.40	191.70	11.44	10.57	15.14	7.24	0.79	8.89	
Gre_Weather_FL				17.49	17.06	17.92	3.45	0.95	3.50	
Gre_Weather_VER				63.98	62.72	65.21	6.26	0.88	6.36	
Mrl_BEST_BB	152.14	146.83	169.62	19.91	16.92	21.10	8.96	0.73	9.42	1.91
Mrl_BEST_FL				24.96	24.26	25.60	5.04	0.83	5.13	2.46
Mrl_BEST_VER				64.45	63.19	65.75	5.91	0.83	5.98	2.44
Mrl_Weather_BB	144.72	142.54	147.71	16.16	15.75	16.65	7.59	0.80	7.71	
Mrl_Weather_FL				17.28	16.84	17.73	4.50	0.87	4.56	
Mrl_Weather_VER				60.35	59.19	61.46	5.50	0.86	5.56	
Mon_BEST_BB	216.56	205.56	217.77	7.64	6.66	12.11	6.67	0.09	6.89	1.05
Mon_BEST_FL				28.04	27.49	28.67	3.18	0.43	3.24	1.32
Mon_BEST_VER				62.07	58.81	65.29	3.97	0.39	4.52	1.28
Mon_Weather_BB	171.13	167.90	184.08	15.42	13.08	16.18	5.65	0.34	6.23	
Mon_Weather_FL				20.34	19.91	20.80	3.01	0.49	3.08	
Mon_Weather_VER				60.43	57.03	63.78	3.58	0.50	4.06	
P-n_BEST_BB	198.53	197.54	221.51	12.98	8.09	13.49	6.28	0.32	7.51	1.22
P-n_BEST_FL				21.85	21.44	22.17	3.33	0.83	3.39	2.39
P-n_BEST_VER				59.50	58.17	60.86	7.11	0.77	7.17	2.07
P-n_Weather_BB	194.18	190.97	197.06	10.27	9.92	10.68	5.02	0.57	5.18	
P-n_Weather_FL				15.29	15.03	15.58	3.35	0.82	3.39	
P-n_Weather_VER				54.53	53.28	55.78	7.06	0.77	7.09	
Rsl_BEST_BB	185.38	181.37	194.30	14.08	13.10	14.89	6.13	0.74	7.01	1.97
Rsl_BEST_FL				22.13	21.59	22.66	3.62	0.91	3.72	3.39
Rsl_BEST_VER				64.63	62.54	66.47	7.96	0.69	8.16	1.79
Rsl_Weather_BB	190.22	183.23	191.45	10.32	10.10	10.95	4.90	0.83	5.53	
Rsl_Weather_FL				15.50	15.13	15.88	3.30	0.92	3.49	
Rsl_Weather_VER				59.88	58.58	61.15	5.34	0.85	7.99	
S-b_BEST_BB	203.48	199.19	207.29	13.06	12.17	14.53	4.22	0.92	4.78	3.62
S-b_BEST_FL				25.34	24.47	26.03	3.41	0.94	3.56	4.04
S-b_BEST_VER				59.27	57.93	60.56	4.80	0.90	4.90	3.16
S-b_Weather_BB	192.22	188.24	195.34	10.26	9.37	11.06	4.97	0.89	6.21	
S-b_Weather_FL				17.76	16.17	19.20	3.20	0.95	3.34	
S-b_Weather_VER				55.16	53.97	56.42	4.77	0.90	4.84	
Syr_BEST_BB	198.63	192.34	204.42	13.55	12.61	14.75	7.22	0.70	7.54	1.83
Syr_BEST_FL				23.91	23.25	24.56	3.79	0.91	3.85	3.40
Syr_BEST_VER				59.99	58.53	61.39	6.55	0.84	6.65	2.52
Syr_Weather_BB	191.43	185.55	196.34	11.05	10.41	12.05	6.68	0.75	7.14	
Syr_Weather_FL				16.88	16.42	17.34	3.55	0.92	3.64	
Syr_Weather_VER				57.19	56.20	58.18	4.77	0.92	4.87	
U-b_BEST_BB	199.74	196.64	219.76	17.80	12.83	18.60	5.33	0.52	6.66	1.45
U-b_BEST_FL				24.41	23.17	25.36	3.80	0.84	4.05	2.46
U-b_BEST_VER				67.36	65.40	69.48	6.80	0.88	6.96	2.92
U-b_Weather_BB	216.88	201.96	230.47	10.18	6.87	13.40	5.39	0.51	8.06	
U-b_Weather_FL				17.23	16.66	17.87	3.19	0.88	3.41	
U-b_Weather_VER				62.47	61.01	63.80	5.07	0.93	5.28	

Table S10. Correlations amongst indicators used to fit bioclimatic envelopes. Results show the average ± standard deviation of correlations computed across 30 GCMs, 30 years (1951-1980), and 11 cultivars at locations utilized to fit their envelopes (see above). Precipitation variables are highly collinear, and yet they differ in their relative importance to determine loss of climatic suitability (see Fig. S17). Temperature-related indicators are not strongly collinear except for minimum and maximum temperatures, but each variable affects winegrape maturation differently.

	Days<10°C	Days>40°C	GDD	GDD>25°C	MaxTemp	MinTemp	MaxPrec	SumPrec
Days<10°C	1.00 ± 0.00	0.01 ± 0.04	-0.61 ± 0.08	-0.16 ± 0.07	-0.61 ± 0.10	-0.79 ± 0.10	0.21 ± 0.25	0.25 ± 0.23
Days>40°C	0.01 ± 0.04	1.00 ± 0.00	0.01 ± 0.03	0.01 ± 0.02	0.00 ± 0.04	-0.00 ± 0.03	0.01 ± 0.06	0.01 ± 0.07
GDD	-0.61 ± 0.08	0.01 ± 0.03	1.00 ± 0.00	0.05 ± 0.01	0.69 ± 0.16	0.68 ± 0.16	-0.14 ± 0.15	-0.19 ± 0.15
GDD>25°C	-0.16 ± 0.07	0.01 ± 0.02	0.05 ± 0.01	1.00 ± 0.00	0.45 ± 0.19	0.55 ± 0.16	-0.12 ± 0.14	-0.19 ± 0.16
MaxTemp	-0.61 ± 0.10	0.00 ± 0.04	0.69 ± 0.16	0.45 ± 0.19	1.00 ± 0.00	0.74 ± 0.11	-0.39 ± 0.17	-0.44 ± 0.17
MinTemp	-0.79 ± 0.10	-0.00 ± 0.03	0.68 ± 0.16	0.55 ± 0.16	0.74 ± 0.11	1.00 ± 0.00	-0.23 ± 0.19	-0.30 ± 0.17
MaxPrec	0.21 ± 0.25	0.01 ± 0.06	-0.14 ± 0.15	-0.12 ± 0.14	-0.39 ± 0.17	-0.23 ± 0.19	1.00 ± 0.00	0.96 ± 0.02
SumPrec	0.25 ± 0.23	0.01 ± 0.07	-0.19 ± 0.15	-0.19 ± 0.16	-0.44 ± 0.17	-0.30 ± 0.17	0.96 ± 0.02	1.00 ± 0.00

Additional Supplemental Figures

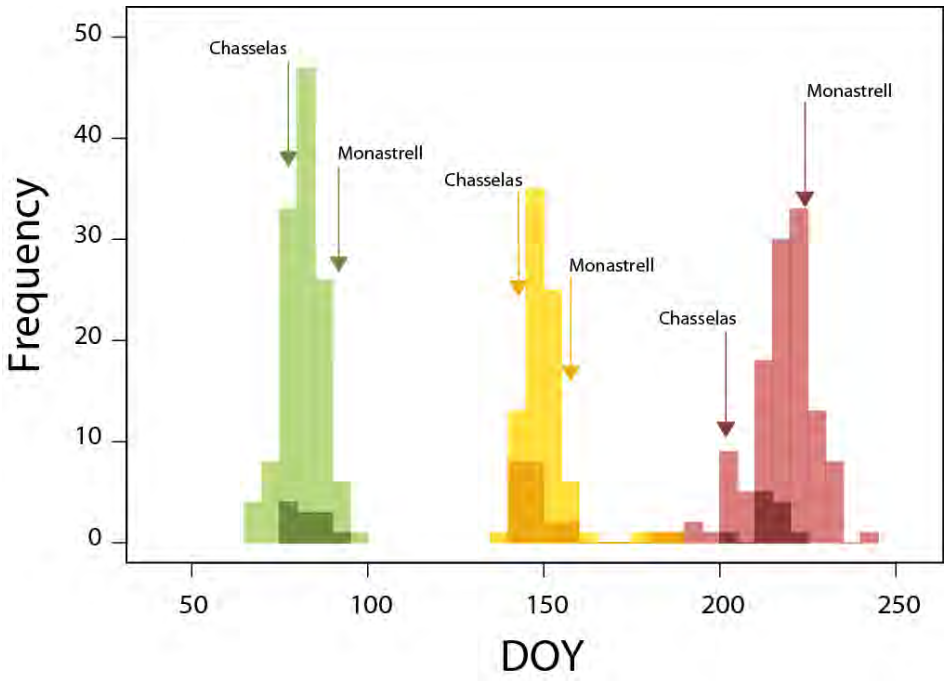

Fig. S4. We selected 11 winegrape cultivars (varieties), ensuring that they span enough diversity in their phenologies. Histograms depict the temporal distribution of the three modeled phenological stages—e.g. budbreak (green), flowering (yellow) and veraison (red)—across 130 varieties included in the Domaine de Vassal collection (lighter colors) and across the 11 varieties analyzed in this study (67). To illustrate the large differences in the phenologies among early and late varieties, we mark the average dates of each phenological stage for two characteristic winegrape varieties known to have either early—Chasselas—or late—Monastrell—phenologies. For more information see *Phenological data for parameterization & validation*.

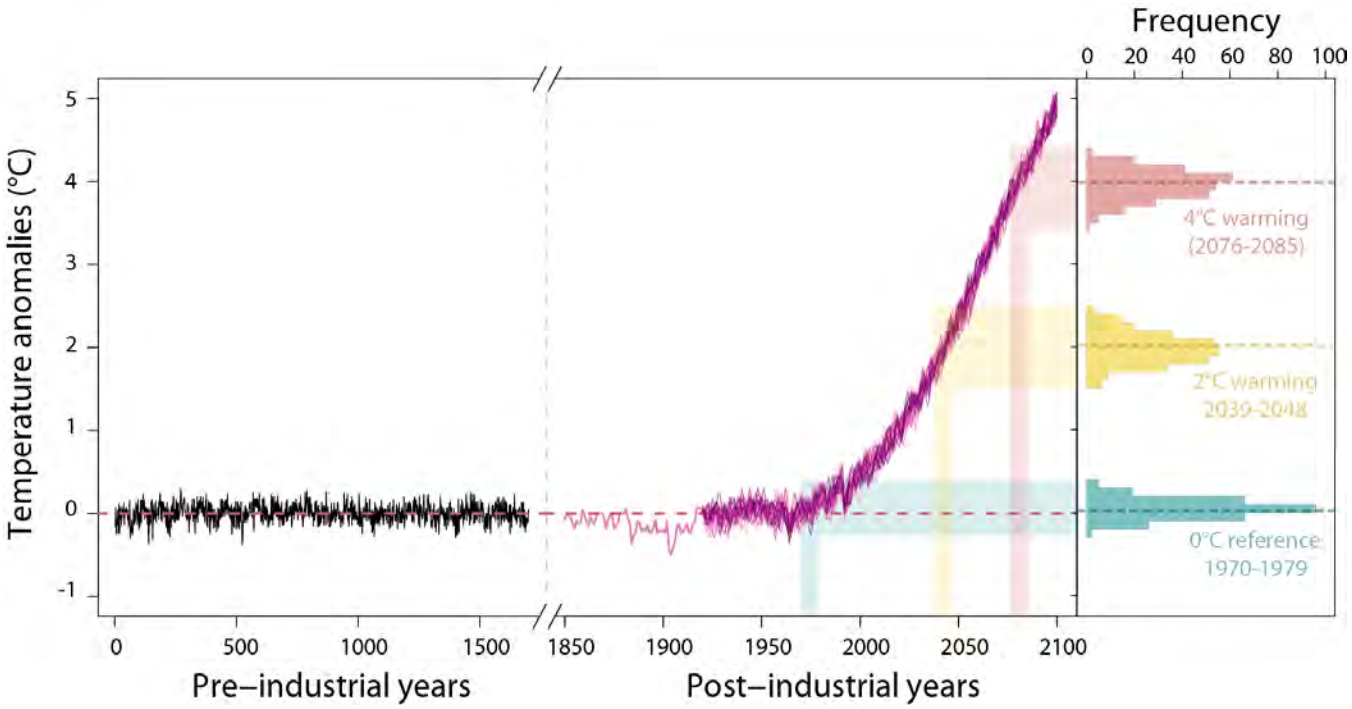

Fig. S5. Evolution of the anomalies in global average temperatures through time. The figure shows global anomalies in temperatures based on 1700 simulations for the pre-industrial era, prior to 1850 (black line), the global average in temperature anomalies for the 1850-1920 period based on one GCM simulation (purple line), and 30 simulated global averages in temperature anomalies for the 1921-2100 period based on 30 GCM simulations (light pink to dark purple lines). We examined two major warming scenarios: 2°C (2039-2048 in RCP 8.5, yellow), 4°C (2076-2085 in RCP 8.5, pink) against a 0°C reference period (1970-1979 in RCP 8.5, blue). Histograms in the right-hand panel show non-overlapping distributions of temperature anomalies across 300 simulations corresponding to each 10 year period and each of the 300 GCM simulations. Dotted lines on top of the histograms represent median values of each distribution of temperatures. The median estimates for the +2°C/+4°C warming scenarios are +2.03/+3.99°C, with interquartile ranges of 1.99-2.06°C and 3.97-4.04°C, respectively.

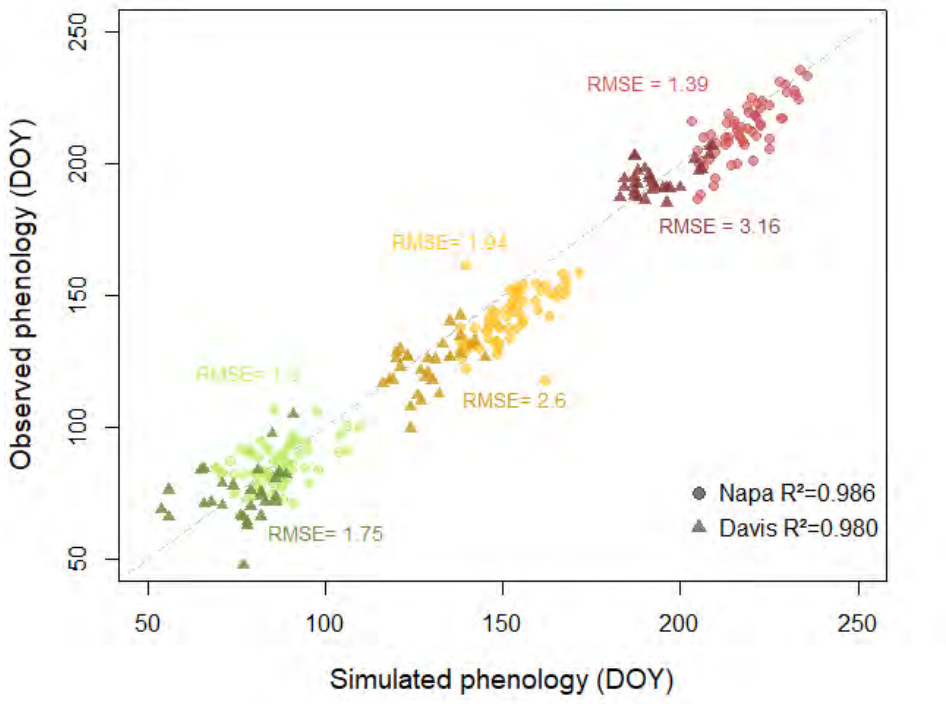

Fig. S6. Phenological modeling validation results comparing simulated dates of phenological stages budbreak (green), flowering (yellow) and veraison (red) for two locations in California (USA), Napa Valley (circles, light colors) and Davis (triangles, dark colors), against independent observations of the phenology therein (8, 9). Observations and simulations comprise the 1985 to 2007 period for Cabernet-Sauvignon, Sauvignon blanc, Chardonnay and Merlot in Napa and the 2014 to 2016 in Davis for all cultivars except for Grenache. Overall regression R^2 are noted for each location across phases and RMSE values for each phenophase and location are marked next to the corresponding cloud of points. Note that error values are rather low, particularly for the Napa dataset.

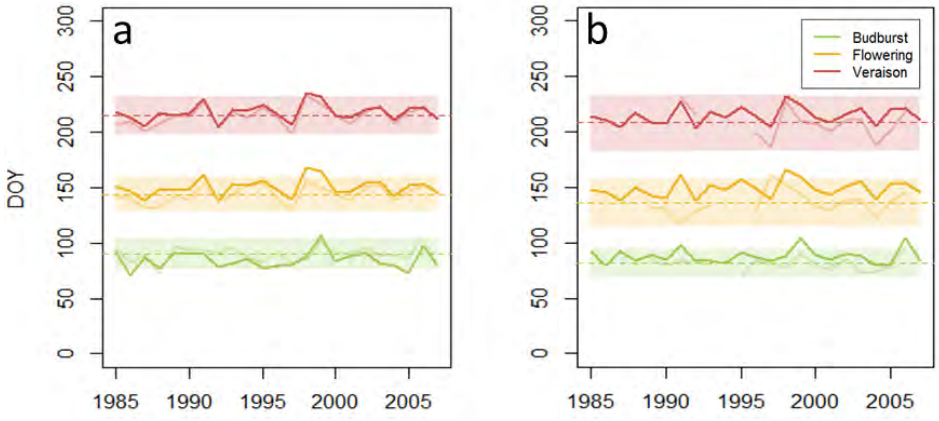

Fig. S7. Example of model validation with independent observations comparing our projections of the phenological stages budbreak (green), flowering (yellow) and veraison (red) for Napa Valley (California, USA) against independent observations therein (8, 9). Results in this example are for Cabernet-Sauvignon (a) and Chardonnay (b). Although projections are based on models calibrated with European data (see above), and thus there are notable differences between climate in the calibration and validation regions, phenological projections (solid lines) closely match the observed phenology (light lines)($r = 0.994$ for Cabernet-Sauvignon; $r = 0.983$ for Chardonnay), and fall within 95% confident intervals for the variation of the observed phenology (shaded areas).

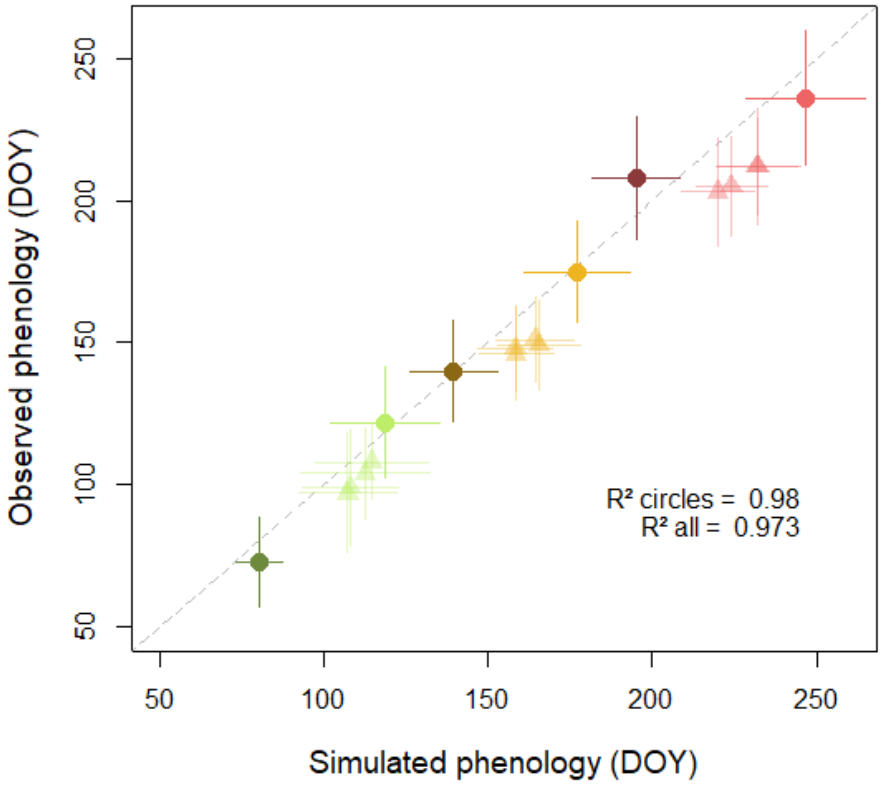

Fig. S8. Phenological modeling validation results comparing our projections of the phenological stages budbreak (green), flowering (yellow) and veraison (red) against independent phenological observations in (5) (light-colored circles), (6) (dark-colored circles), and (7) (light-colored triangles). The different symbol used for the Ruml *et al.* (2016) data stems from it reporting an earlier phenological stage than we modeled. Results show an overall strong correlation between observed phenology and the phenology simulated by phenological models. Error bars represent 95% CI around the mean.

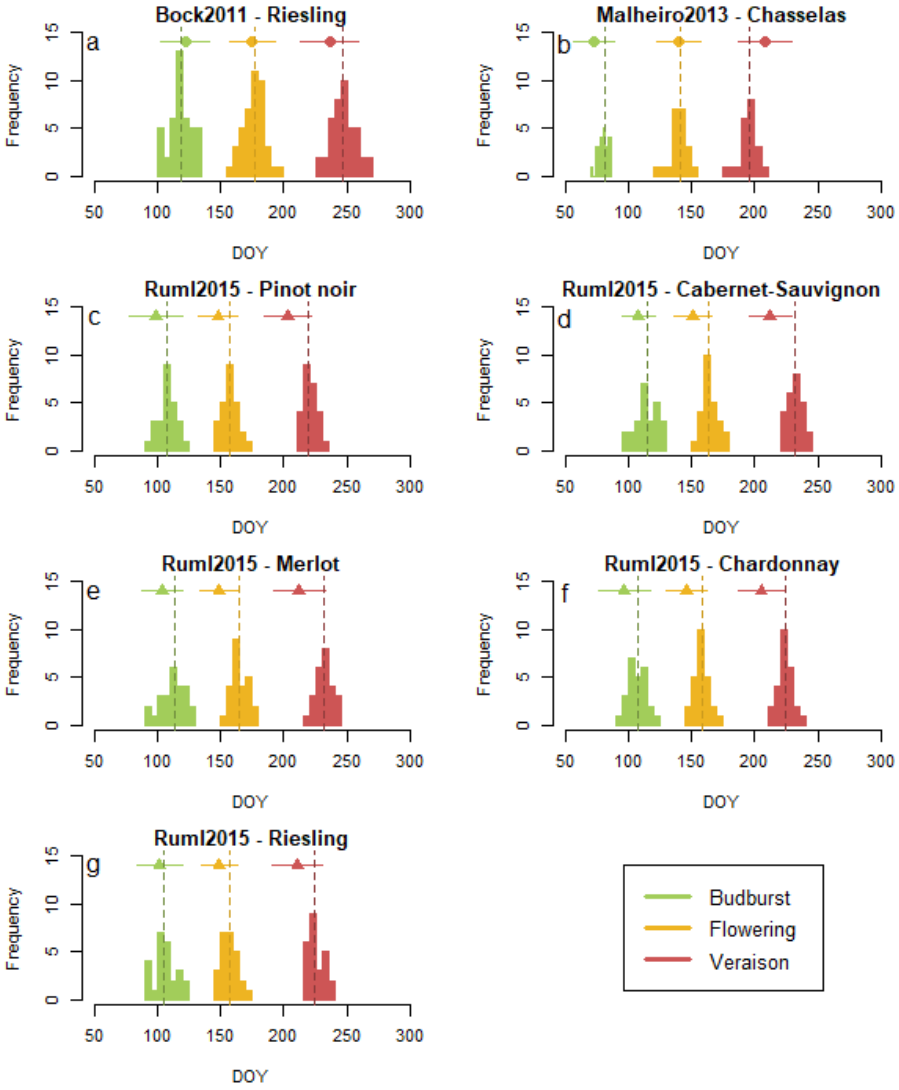

Fig. S9. Phenological modeling validation results comparing our projections of the phenological stages budbreak (green), flowering (yellow) and veraison (red) against independent observations in published work (5–7). The histograms summarize our phenological projections across the time period during which independent observations were recorded. The circles and triangles above the histograms represent the means and their error intervals represent the 95% confident intervals of observed phenology. Note that our projections for winegrape phenology consistently predict later than observed phenology for the Ruml *et al.* (2016) dataset, given that their results are for earlier stages than those parameterized by our models. This is the reason for the use of triangles instead of circles. Results in this example are for Riesling (a,g), Chasselas (b), Pinot noir (c), Cabernet-Sauvignon (d), Merlot (e), Chardonnay (f).

Fig. S10. Geographical locations utilized to model maturity for each of the 11 winegrape varieties analyzed in this study. Locations are marked by red dots and were extracted from (3), see also *Modeling maturity*.

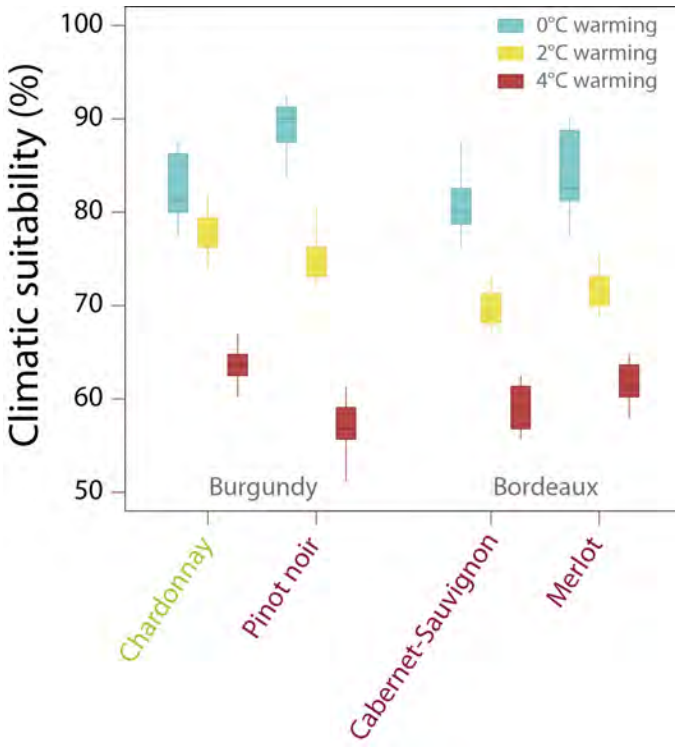

Fig. S11. Estimated climatic suitability for regions including Bordeaux and Burgundy under our 0°C reference scenario, 2°C, and 4°C warming scenarios. Our metric of suitability incorporates uncertainty in the climate that determines whether a location is good for growing a particular variety every year. Thus, suitability below 100%, in part, highlights that every year is not always ideal for a variety in a region (68). See also *Calculating climatic suitability*.

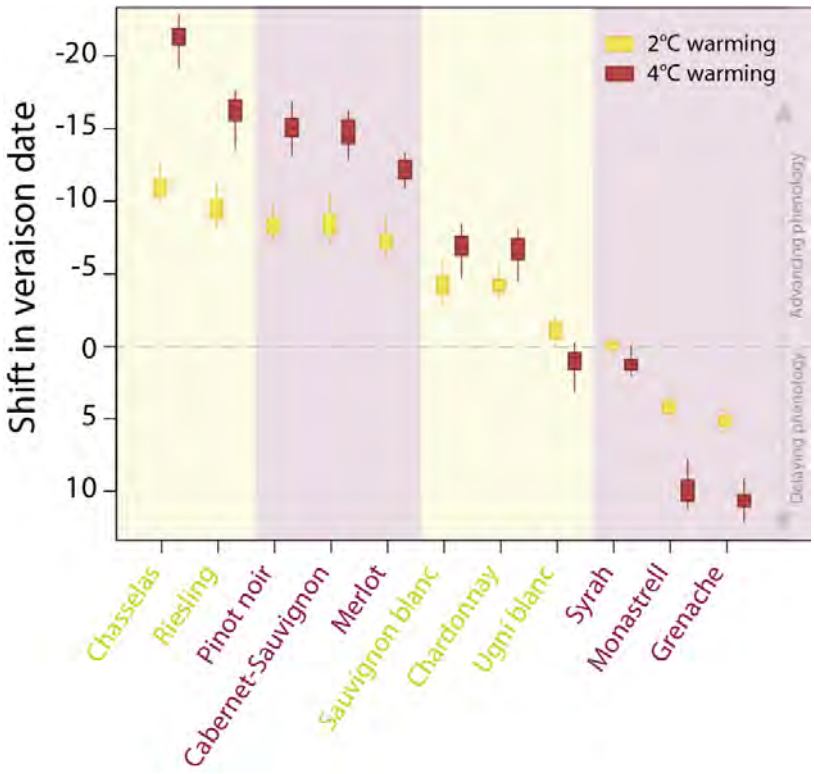

Fig. S12. Variation in the predicted shifts in phenology across the 11 winegrape varieties in our dataset. Shifts in phenology are shown for two warming scenarios: 2°C (yellow) and 4°C (red), and are calculated by comparing predicted veraison dates under these scenarios against predicted veraison during the 0° reference scenario. Winegrape varieties are ranked according to the magnitude of the veraison shifts.

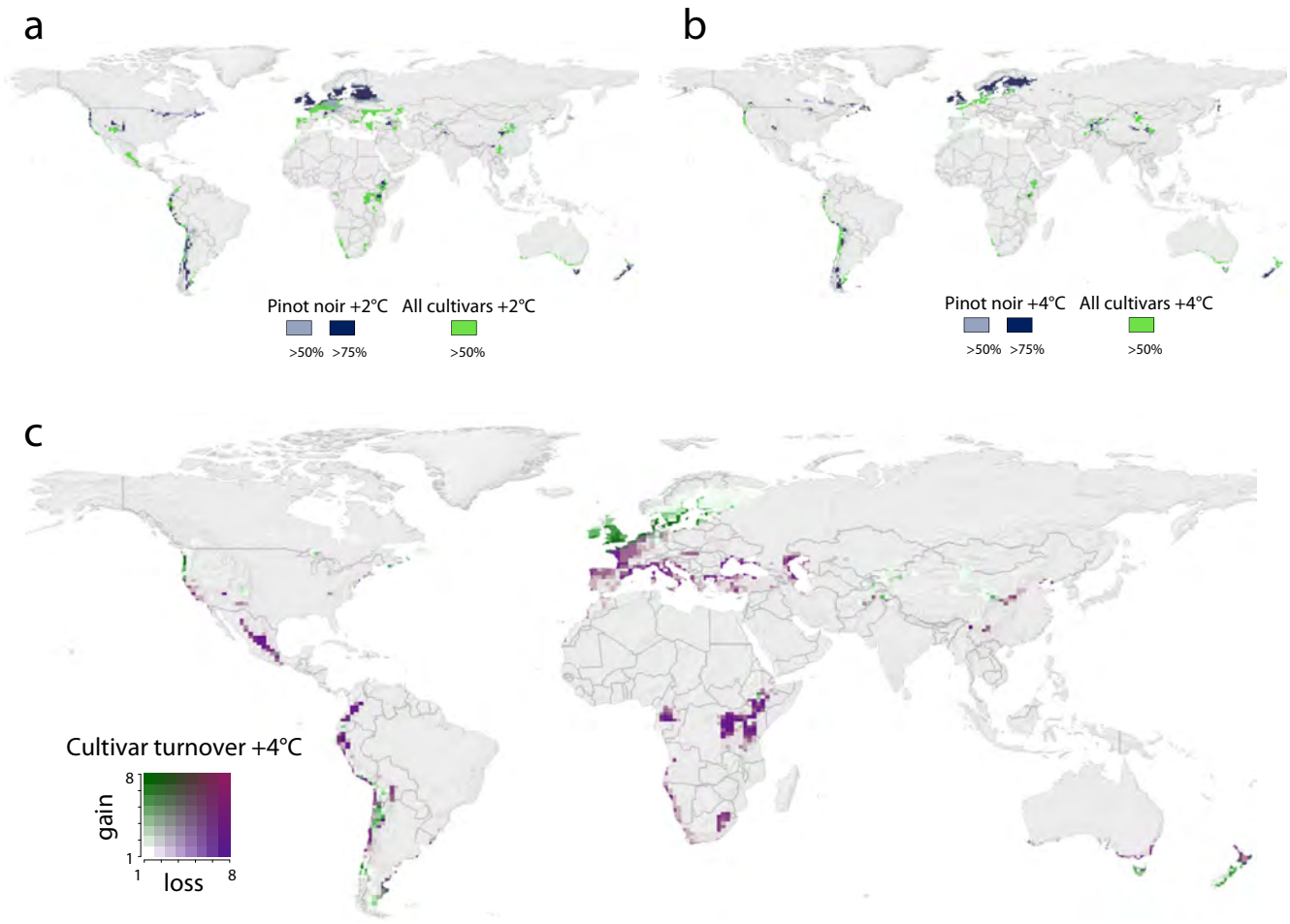

Fig. S13. Predicted effects of climate change on cultivar (variety) distribution. Panel (a) depicts the predicted areas suitable to grow Pinot noir under different levels of climatic suitability (over 50% and 75%) and areas of the globe our model predicts are climatically suitable for the remaining varieties, for a 2°C warming scenario. Similarly, panel (b) shows predicted suitable areas for Pinot noir vs. other varieties under the 4°C warming scenario. Panel (c) shows in a bivariate color scale simultaneously variety gains (white to green) and losses (white to purple) predicted under 4°C of warming. Climatic suitability is defined as the percentage of model-years (i.e., 300 years: 10 years x 30 ensemble members) when our modeling approach suggested a variety would reach maturity in a region (see above for details). Note that both gains and losses of climatic suitability (c) are calculated with respect to areas projected to be suitable under the 0°C, and thus, do not refer to current growing regions (see Fig. S1).

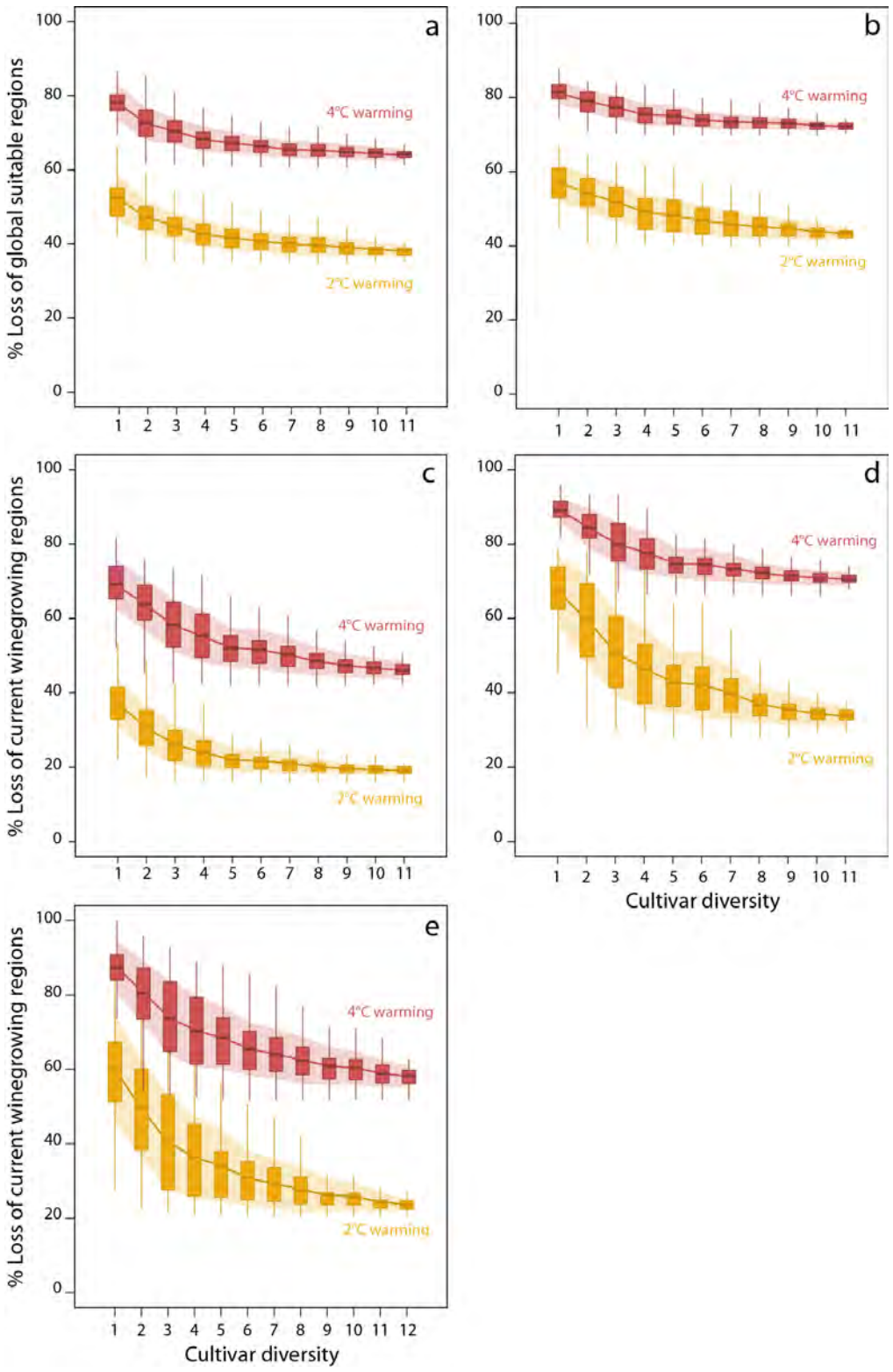

Fig. S14. Alternative analyses of the proportion of climatic suitability losses versus winegrape cultivar diversity (see also main text Fig. 2). Panels show decrease in loss of suitable regions with increasing diversity for both a scenario of 2°C warming (yellow bars) and one of 4°C warming (red bars) for: (a) all global regions potentially suitable for winegrowing using all 8 climatic variables, (b) all global regions potentially suitable for winegrowing using temperature variables only, (c) current growing regions excluding maximum and minimum temperatures, (d) current growing regions using temperature variables only and, (e) current growing regions using all 8 climatic variables and including the Late-ripening composite variety and thus, 12 winegrape varieties. Shaded areas illustrate ± 1 standard deviation around the mean climatic suitability loss for the corresponding number of sampled varieties.

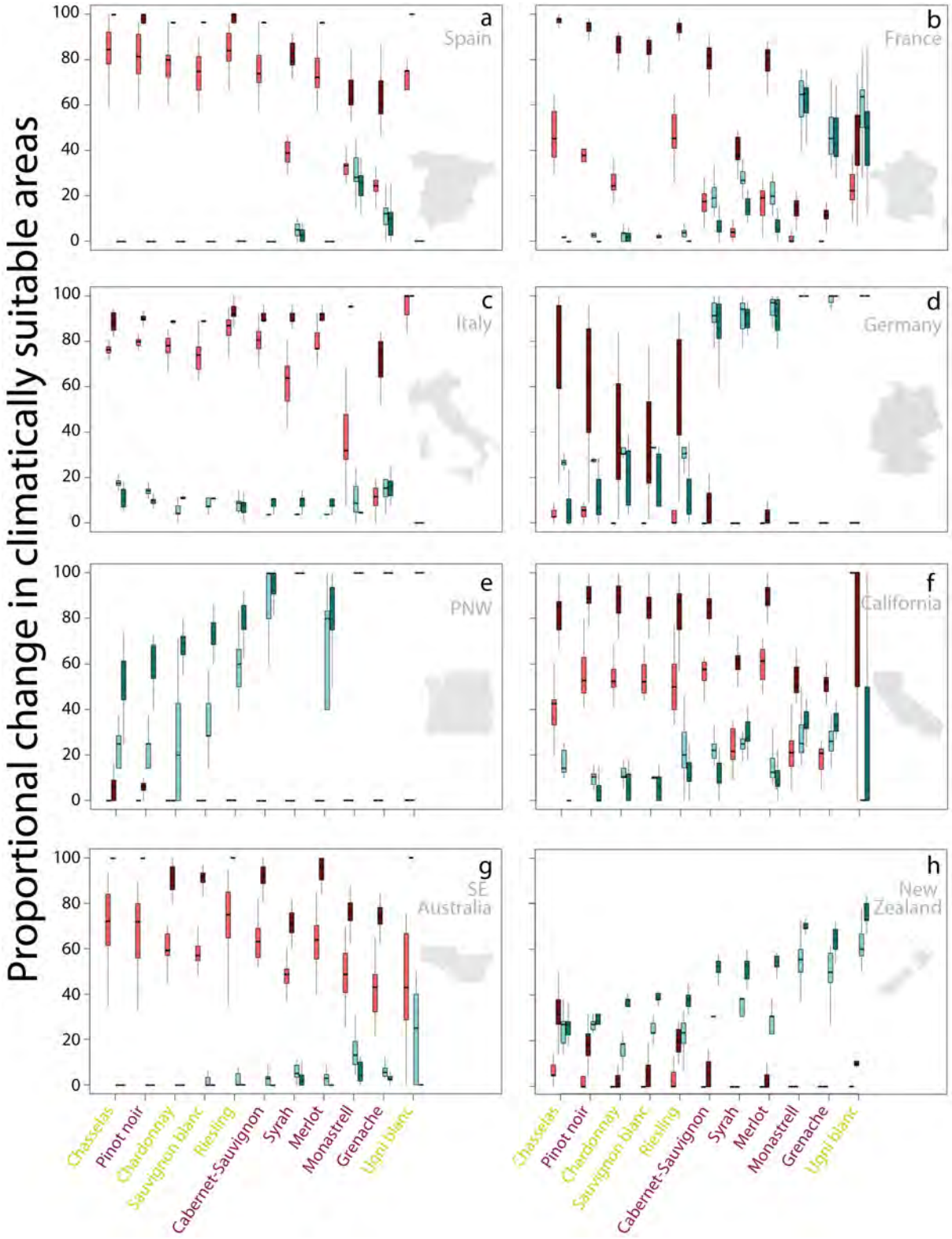

Fig. S15. Shifts in predicted climatic suitability for 11 studied varieties within 8 popular winegrowing regions (see also main text Fig. 3), including Spain (a), France (b), Italy (c), Germany (d), Pacific Northwest (USA) (e), California (USA) (f), South Eastern Australia (g) and New Zealand (h). Increases in suitability are represented by light turquoise (2°C warming) and dark turquoise (4°C degree warming) colors, and suitability decreases by light red (2°C warming) and dark red (4°C warming). Winegrape varieties are ranked according to their phenological order, following (2). Note that these estimates are based on modelled suitability and thus we may show low suitability for some varieties already grown in some regions (see *Calculating climatic suitability* in main text for more information).

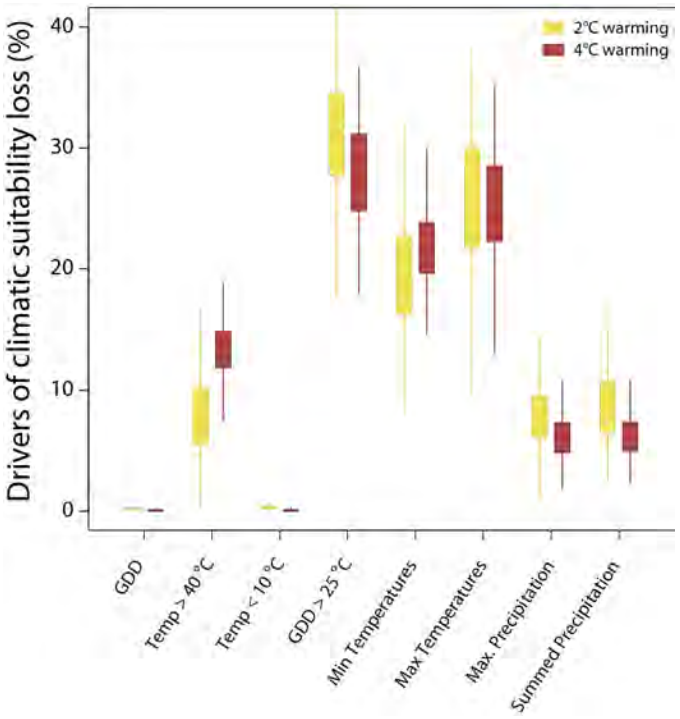

Fig. S16. Drivers of loss of climatic suitability within current winegrowing regions. Results for all eight climatic variables included as predictors in the bioclimatic envelopes (see *Modeling maturity*). Estimates were calculated as a proportion of losses for all varieties under scenarios of warming of 2°C (yellow bars) and 4°C (red bars). Error bars show variation in the proportion of losses due to each climatic variable across GCMs and years.

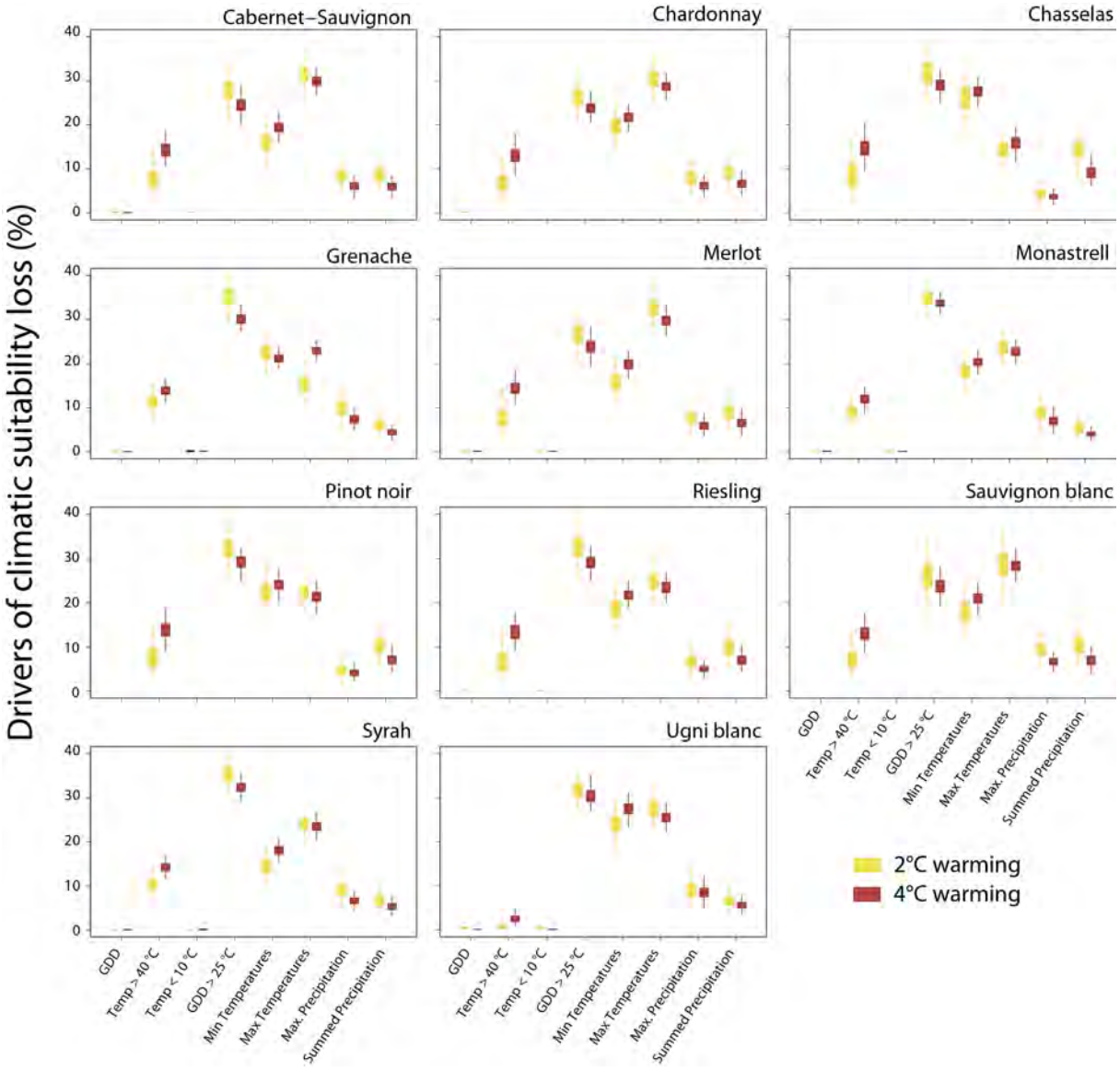

Fig. S17. Drivers of loss of climatic suitability within current winegrowing regions. Results for all eight climatic variables included as predictors in the bioclimatic envelopes to model climatic suitability to reach maturity. Estimates were calculated as a proportion of losses for each of the 11 studied varieties under scenarios of warming of 2°C (yellow bars) and 4°C (red bars). Error bars show variation in the proportion of losses due to each climatic variable across GCMs and years. Note that we do not show loss due to the veraison date cut-off, as no regions were lost due to this at 2°C, and at 4°C less than 1% of regions were lost for all varieties, except for Ugni blanc, which lost 2% of regions to veraison after October 1.

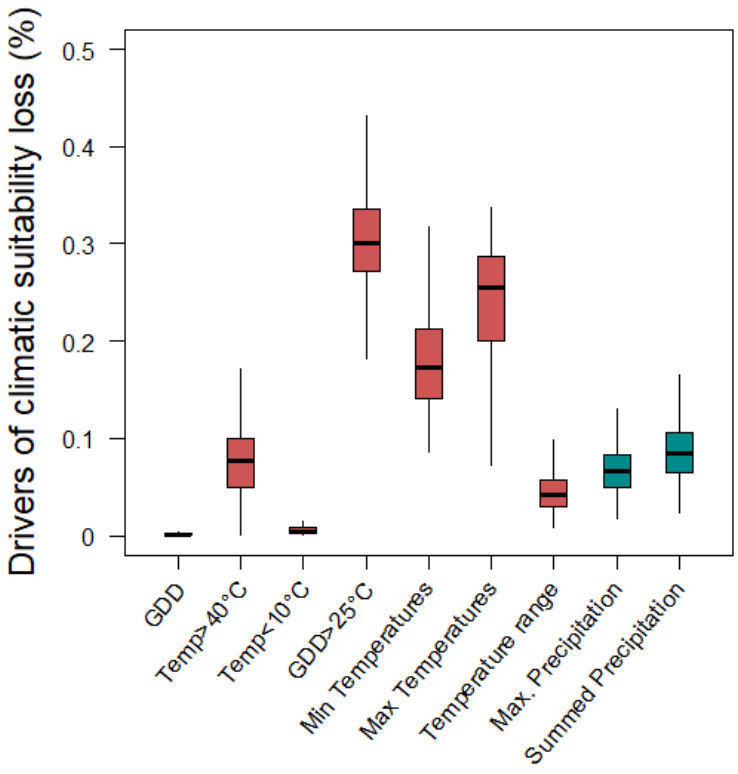

Fig. S18. Sensitivity analysis of the drivers of loss of climatic suitability within current winegrowing regions, including the influence of Diurnal Temperature Range amongst the temperature-related predictors (red bars). Results for all nine climatic variables included as predictors in the bioclimatic envelopes (see *Modeling maturity* and *Sensitivity analysis for Diurnal Temperature Range*). Estimates were calculated as a proportion of losses for all varieties under scenarios of warming of 2°C. Error bars show variation in the proportion of losses due to each climatic variable across 5 randomly selected GCM simulations (see above) and the 10 years corresponding to each 0°C and 2°C scenario for which region loss is computed.

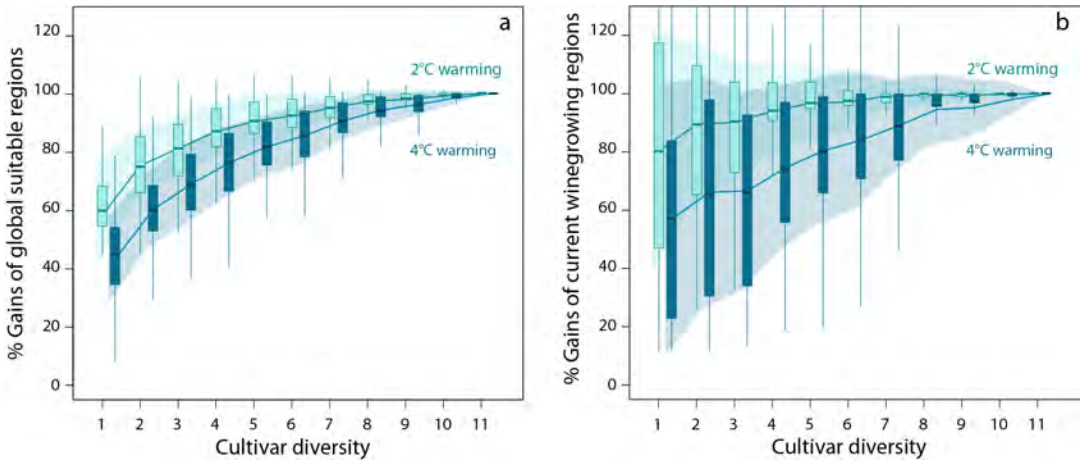

Fig. S19. Proportion of climatic suitability gains calculated across all potential climatically suitable regions of the world (a) and within current winegrowing regions (b), versus winegrape cultivar diversity, out of maximum suitability gains by the 11 varieties. Predictions of climatic suitability gains are shown for both a scenario of 2°C warming (green bars) and one of 4°C warming (blue bars). Depicted uncertainty shows variability in climatic suitability losses according to all possible combinations of *n* varieties, and their modelled suitability under each climate change scenario. Shaded areas illustrate +/- 1 standard deviation around the mean climatic suitability gains for each number of varieties.

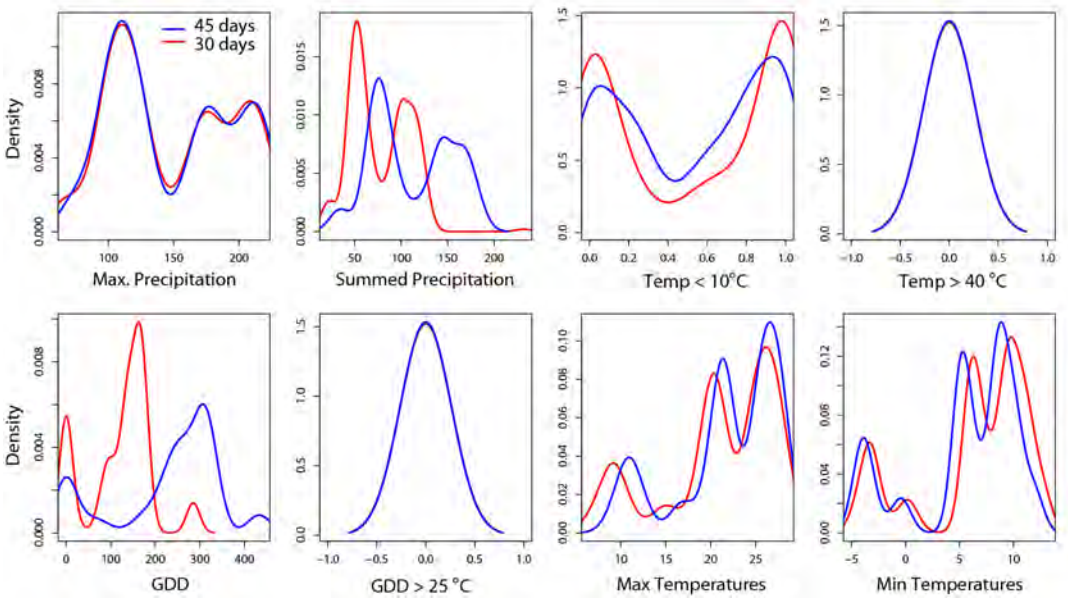

Fig. S20. Density plots comparing the distribution of values corresponding to each of the eight climatic variables utilized to fit climatic envelopes, recorded either over a 45-day period after veraison (blue) or over a 30-day period after veraison (red) for Chasselas across the 19 locations selected to fit the envelopes for this variety.

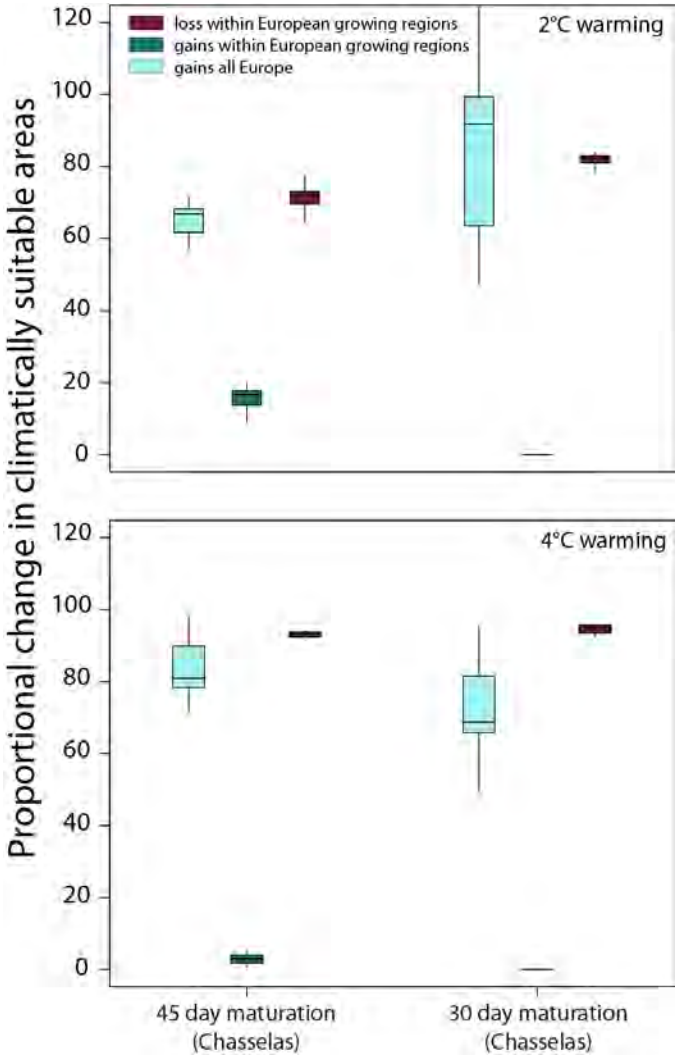

Fig. S21. Shifts in predicted climatic suitability for Chasselas in Europe (see also main text Fig. 3), according to climatic envelopes computed over either a 45-day period after veraison (left) or a 30-day period after veraison (right). Increases in suitability across all of Europe are represented by light green boxes, increases within current growing regions (see Fig. S1) are represented by dark green boxes, and decrease in climatic suitability within those regions are represented by dark red boxes. Both estimates of suitability gains and losses are presented for two warming scenarios, 2°C warming (above) and 4°C warming (below).

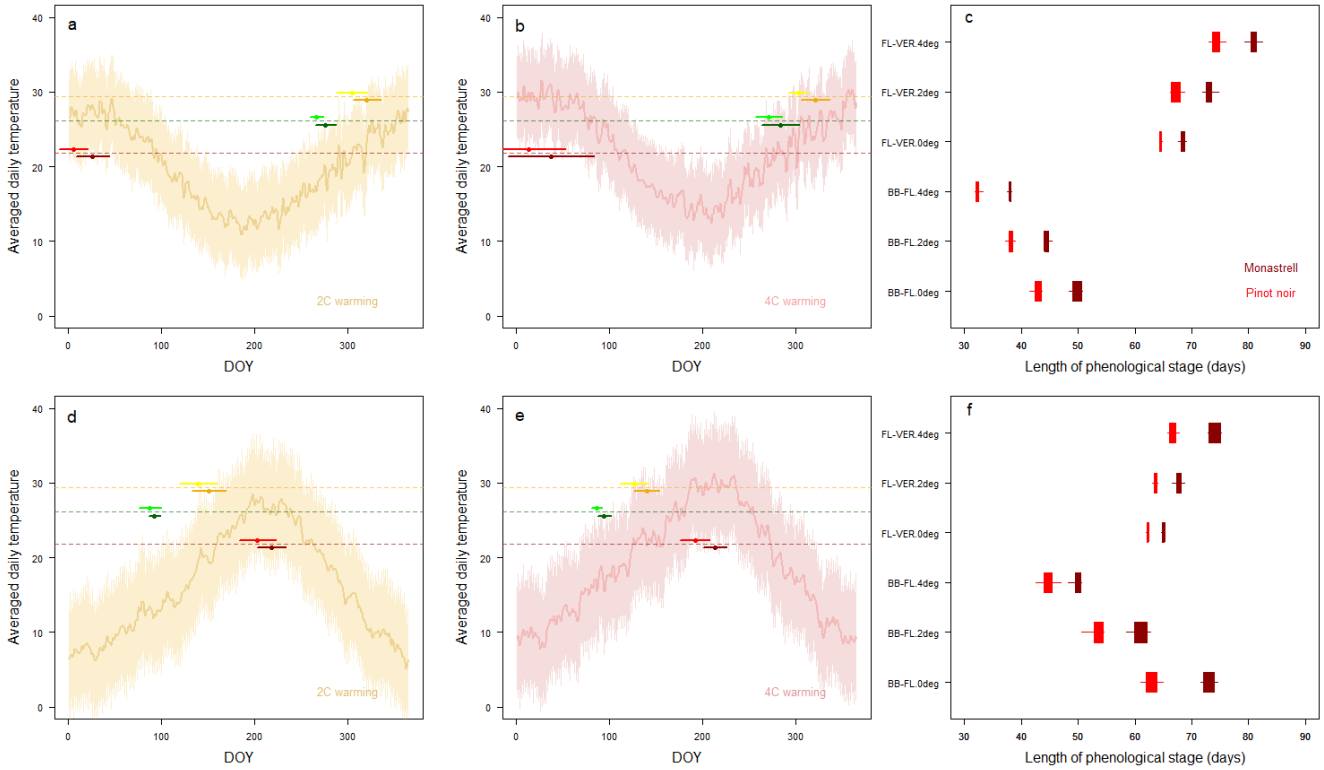

Fig. S22. Drivers of phenological advances and delays. Our analyses show that some winegrape cultivars with late phenology (e.g., Monastrell and Grenache; see Fig. S12) have delays in veraison under warming scenarios. In our non-linear phenological models, delays are expected when the temperatures experienced during a given phenological stage are above the optimal parameterized temperature for that stage (T_{opt}, shown here as dashed lines). The panels illustrate average daily temperatures for two example countries, Australia (a,b) and Spain (d,e), under the two warming scenarios of 2°C (yellow; a,d) and 4°C (red; b,e). Dates of predicted phenology are shown for budbreak (BB, green), flowering (FL, yellow) and veraison (VER, red) for Pinot noir, a variety with early phenology (lighter colors) and a variety with late phenology, Monastrell (darker colors), which often shows delayed phenology in our higher warming scenario (4°C). Delays are expected only when temperatures are above the parameterized optimum values (dashed lines). Thus, in both countries (c,f) the period between budbreak and flowering shortens as climate warms (BB-FL) because warming increases temperatures, but (in these cases) never beyond the parameterized optimum values (dashed lines). In contrast, the period of flowering to veraison (FL-VER) lengthens as climate goes from 0°C to 4°C warming (c,f), and temperatures are often higher than the fitted optimums- this leads to delaying phenology. This is seen in our models most commonly for late varieties such as Monastrell and Grenache because they take longer to move through phenological stages (because of their high requirements of forcing accumulation, F*) – and thus experience the higher temperatures longer than early-ripening varieties.

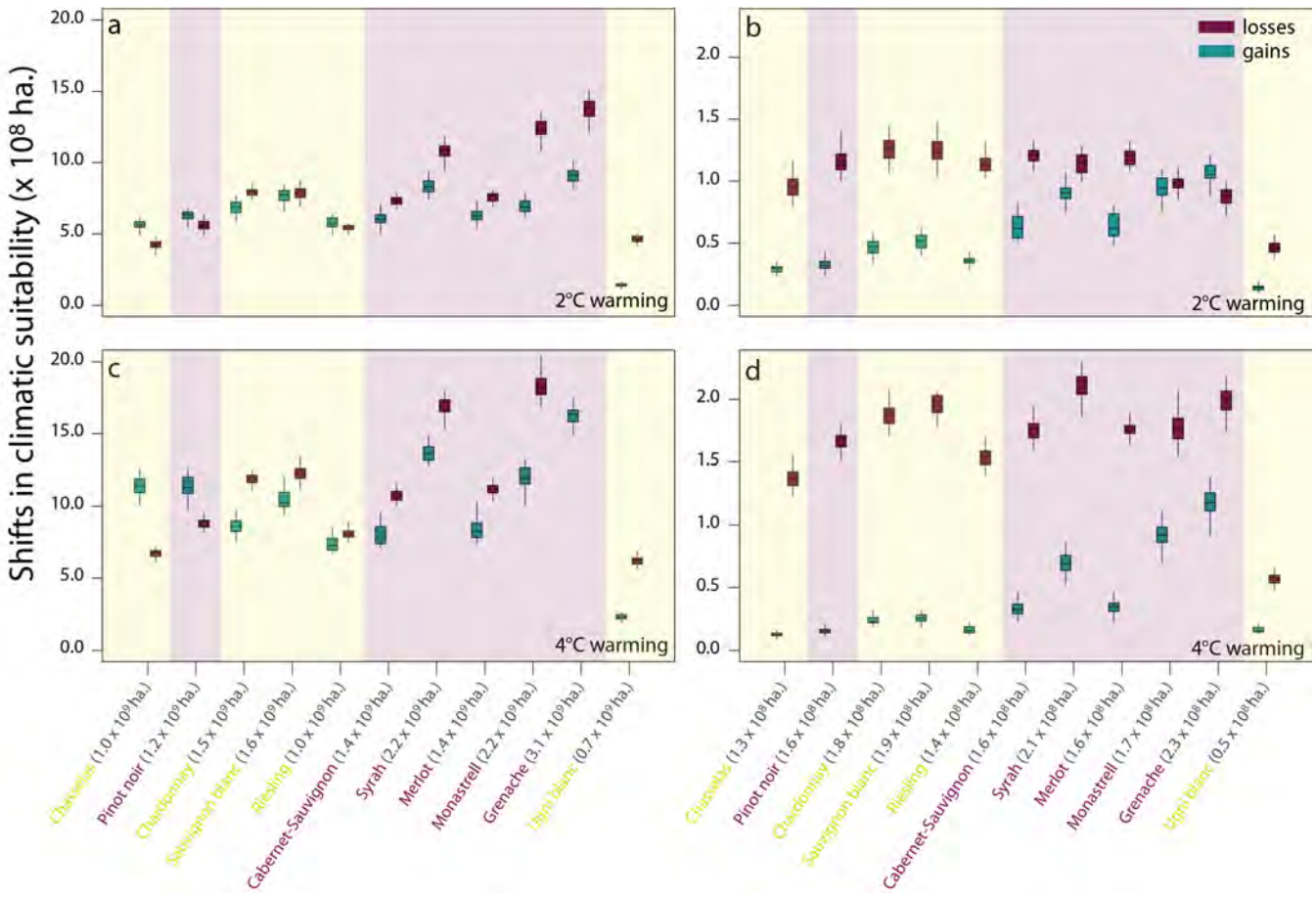

Fig. S23. Predicted gains (turquoise) and losses (purple) of climatically suitable growing areas for each of the 11 studied winegrape varieties (cultivars) under scenarios of (a, b) 2°C and (c, d) 4°C warming. We show gains and losses as absolute values (in hectares) for each variety with warming (i.e., the area predicted with warming relative to the area predicted under our reference scenario of 0°C). Both gains and losses are calculated relative to areas identified as climatically suitable under our reference scenario both globally (a, c) and within current winegrowing regions (b, d). Values in parenthesis in the x-axes report the amount of hectares with suitable climate to grow each variety under the 0°C reference scenario. These values differ among panels as suitable hectares are computed either across all the world (a, c) or within current growing regions (b, d). Note that both gains and losses computed for global suitable areas (a, c) should not be interpreted as actual gains or losses of suitability for winegrowing but as potential ones if winegrapes had been planted in all climatically suitable regions of the planet in our reference scenario of 0°C. Background shading and variety name coloring differentiates red from white varieties.